MULTI MATERIAL TOPOLOGY OPTIMIZATION WITH HYBRID CELLULAR AUTOMATA

A Thesis

Submitted to the Faculty

of

Purdue University

by

Jennifer Solis Ocampo

In Partial Fulfillment of the

Requirements for the Degree

of

Master of Science in Mechanical Engineering

August 2017

Purdue University

Indianapolis, Indiana

THE PURDUE UNIVERSITY GRADUATE SCHOOL
STATEMENT OF COMMITTEE APPROVAL

Dr. Andres Tovar, Chair

Department of Mechanical Engineering

Dr. Alan Jones

Department of Mechanical Engineering

Dr. Hazim El-Mounayri

Department of Mechanical Engineering

Approved by:

Dr. Sohel Anwar

Chair of the Graduate Program

To my parents and my brother. Los amo. Asi de simple, porque significan tanto para mi que no creo que se le deban agregar adjetivos al amor.

ACKNOWLEDGMENTS

First of all to God, for his grace and love over these two years. I thank my family for supporting me and motivating me to accomplish my goals, even if that means being away from home. A special thanks to Dr. Tovar for his vocation for teaching, for all the shared knowledge, and for believing in my capability. Thanks to Dr. El-Mounayri and Dr. Jones for their kind support and interest in this work. To Homero, for his loyal friendship, and his company in good and not so good moments. To my fellows from lab for their solidarity and good spirit.

TABLE OF CONTENTS

Page

LIST OF TABLES vii

LIST OF FIGURES viii

ABBREVIATIONS xi

ABSTRACT xiii

1 INTRODUCTION 1

1.1 Topology Optimization Problem 2

1.2 Design Variable Approaches 2

1.3 Optimizers or updating schemes 4

1.4 Numerical Instabilities 5

1.5 Density Approach 6

1.6 Hybrid Cellular Automaton Algorithm (HCA) [18] 7

1.7 Objective 14

2 MULTI MATERIAL TOPOLOGY OPTIMIZATION 16

2.1 Current approaches 16

2.2 Alternating Active Phase Algorithm [12] 18

2.3 Ordered SIMP Algorithm [32] 20

3 CRASHWORTHINESS TOPOLOGY OPTIMIZATION 24

3.1 Current approaches 24

3.2 HCA for Crashworthiness Topology Optimization [37] 26

3.3 Crashworthiness Multi Material Topology Optimization 30

4 EVALUATION OF MMTO ALGORITHMS 31

4.1 Alternating Active Phase 33

4.2 Ordered SIMP 41

5 HCA FOR MULTI MATERIAL TOPOLOGY OPTIMIZATION 49

Page

5.1 Algorithm 50
5.1.1 Interpolation function 50
5.1.2 Update rule 51
5.1.3 Volume constraint 52
5.2 Numeric examples for static loading 54
6 HCA FOR MULTI MATERIAL CRASHWORTHINESS TOPOLOGY OPTIMIZATION 63
6.1 Algorithm 63
6.2 Ls Dyna Integration 66
6.3 Numeric examples for dynamic loading 68
6.3.1 Beam under transverse impact 70
6.3.2 Bumper under transverse impact 76
6.3.3 Design time influence in the design solution 81
7 SUMMARY AND RECOMMENDATIONS 84
REFERENCES 86

LIST OF TABLES

Table Page

4.1 Active Phase Simulation Parameters 33

4.2 Ordered SIMP Simulation Parameters 41

5.1 HCA Simulation Parameters for static simulations 55

6.1 HCA Simulation Parameters for impact simulations 68

6.2 Ls Dyna Simulation Parameters for impact simulations 70

LIST OF FIGURES

Figure Page

1.1 Two dimensional neighborhoods for CA. (a)Empty (b)Von Neumann (c)Moore (d)Extended 8

1.2 Two dimensional boundary conditions for CA. (a) Fixed (b) Adiabatic (c) Reflecting (d) Periodic. 9

2.1 Interpolation curves for modulus of elasticity and cost for a monotonic three phases optimization. 23

2.2 Possible cases of interpolation function for two materials. 23

3.1 4 Stress-strain curve for inelastic events. The area under the curve represents the dissipated energy. [37] 27

4.1 Simulation boundary conditions. 32

4.2 Designs for MBB using Alternating Active Phase (a)Mesh of 60x20 (b) Mesh of 150x50. 34

4.3 SED function convergence for MBB using Alternating Active Phase. 35

4.4 Normalized resolution error for MBB using Alternating Active Phase. . . . 36

4.5 Density distribution for MBB using Alternating Active Phase. 37

4.6 Designs for BIW using Alternating Active Phase (a)Mesh of 60x20 (b) Mesh of 150x50. 37

4.7 SED function convergence for BIW using Alternating Active Phase. 38

4.8 Normalized resolution error for BIW using Alternating Active Phase. . . . 39

4.9 Density distribution for BIW using Alternating Active Phase. 40

4.10 Designs for MBB using Ordered SIMP (a)Mesh of 60x20 (b) Mesh of 150x50.42

4.11 SED function convergence for MBB using Ordered SIMP. 43

4.12 Normalized resolution error for MBB using Ordered SIMP. 44

4.13 Density distribution for MBB using Ordered SIMP. 45

4.14 Designs for BIW using Ordered SIMP (a)Mesh of 60x20 (b) Mesh of 150x50.45

4.15 SED function convergence for BIW using Ordered SIMP. 46

Figure Page

4.16 Normalized resolution error for BIW using Ordered SIMP. 47

4.17 Density distribution for BIW using Ordered SIMP. 48

5.1 Interpolation function for design variable and material properties. 51

5.2 Simulation boundary conditions. 55

5.3 Designs for MBB using MMTO HCA (a)Mesh of 60x20 (b) Mesh of 150x50. 56

5.4 SED function convergence for MBB using MMTO HCA. 57

5.5 Normalized resolution error for MBB using MMTO HCA. 58

5.6 Density distribution for MBB using MMTO HCA. 59

5.7 Designs for BIW using MMTO HCA (a)Mesh of 60x20 (b) Mesh of 150x50. 59

5.8 SED function convergence for BIW using MMTO HCA. 60

5.9 Normalized resolution error for BIW using MMTO HCA. 61

5.10 Density distribution for BIW using MMTO HCA. 62

6.1 Dynamic simulation boundary conditions. 69

6.2 Prescribed displacement for pole (rigid wall). 70

6.3 Cantilever beam under impact load using MMTO HCA. The design on the left side corresponds to the 2D Matlab model and design on the right to the 3D Ls Dyna model. 72

6.4 Normalized resolution error for cantiliver beam using MMTO HCA. 73

6.5 Density distribution for cantilever beam under transverse impact using MMTO HCA.. 73

6.6 Convergence for cantilever beam under transverse impact using MMTO HCA. 74

6.7 SED distribution for the cantilever beam under impact load using MMTO HCA. 75

6.8 Bumper under impact load. The design on the left side corresponds to the 2D Matlab model and the two designs on the right to the 3D Ls Dyna model.77

6.9 Normalized resolution error for half bumper using MMTO HCA. 78

6.10 Density distribution for half bumper under transverse impact using MMTO HCA.. 78

6.11 Convergence for half bumper under transverse impact using MMTO HCA. 79

Figure Page

6.12 SED distribution for half bumper under impact load using MMTO HCA. . 80

6.13 Cantilever beam under impact load for different design times. The design on the left side corresponds to the 2D Matlab model, and design on the right to the 3D Ls Dyna model. 82

6.14 Objective function convergence for different impact velocities 83

ABBREVIATIONS

BIW:	Body in White
CA:	Cellular Automaton
CONLIN:	Convex Linearization (method)
ESL:	Equivalent Static Loads
ESO:	Evolutionary Structural Optimization
FE:	Finite Element
FEA:	Finite Element Analysis
HCA:	Hybrid Cellular Automaton
IRM:	Inertia Relief Method
ISE:	Isotropic Solid or Empty
LP:	Linear Programing
LSM:	Level Set Methods
MBB:	Messerschmitt-Blkow-Blohm (beam)
MMA:	Method of Moving Asymptotes
MMTO:	Multi Material Topology Optimization
OC:	Optimal Criteria Method
PD:	Proportional Derivative (control)
PID:	Proportional Integral Derivative (control)
RSM:	Response Surface Method
SED:	Strain Energy Density
SIMP:	Solid Isotropic Material with Penalization
SLP:	Sequential Lineal Programming
SQP:	Sequential Quadratic Programming

SP:	Set Point
TO:	Topology Optimization

ABSTRACT

Solis Ocampo, Jennifer M.S., Purdue University, August 2017. Multi Material Topology Optimization with Hybrid Cellular Automata. Major Professor: Andres Tovar.

Topology Optimization is a technique that allows for the obtaining structures which maximize the use of the material. This is done by intelligently deciding the binary distribution of solid material and void, in a discretized given space. Several researchers have provided methods to tackle binary topology optimization. New efforts are focused on extending the application for multi-phase optimizations. At the industrial level, several components designed are made up of more than one material to reduce weight and production costs. The objective of this work is to implement the algorithm of Hybrid Cellular Automaton for multi-material topology optimization. The commonly used interpolation rule SIMP, which allows to relate the design variables to the mechanical properties of the material, is replaced by ordered SIMP interpolation function. The multiple volume constraints are applied sequentially, starting with the most elastic material. When a constraint is satisfied, the elements assigned to this material remain passive by a defined number of iterations to promote the convergence of the solution. Examples are shown for static and dynamic loads. The work demonstrates the versatility of algorithms based on control systems to solve problems of multiple phases and transient response fields.

1. INTRODUCTION

Topology Optimization (TO) is an optimization problem that seeks for an optimal distribution of material within a design space, so that, under certain design constraints and loading conditions, a given response is minimized. The distribution of material (arrangement and quantity) has a direct effect on the mechanical, thermal and electrical performance of a component. For this reason, there is one (or more) material distributions that favor the component response, which correspond to the global or local minimum of the response function. TO opens the perspective for more organic and complex designs that may be difficult to obtain through an iterative design process.

Structures subjected to static loading conditions are the most common problem solved in topology optimization. For these cases, the objective function to be minimized may include the maximum displacement, stress distribution, compliance, among others. The design constraints correspond to the requirement that the design must comply. Among the most common are maximum total mass and design physical boundaries for structural optimization. The maximum total mass is usually expressed as a percentage of the total possible mass within the design space. To compute the response of the component, the design domain is discretized using Finite Element Analysis (FEA). The element type will depend on the problem formulation.

1.1 Topology Optimization Problem

The structural optimization problem is formulated as:

$$\begin{aligned} \underset{x}{\text{minimize}} \quad & f(x_i) \\ \text{subject to} \quad & \frac{\sum_{i=1}^{nele} x_i}{nele} \leq M_f \\ & 0 \leq x_i \leq 1 \end{aligned} \tag{1.1}$$

Where, F is the objective function to be minimized; x corresponds to the design variable, in this case, the elemental densities; N is the number of elements in the design domain; V is the design constraint, commonly used volume fraction. The density is restricted to assume values of zero or one, which represent void or solid material. Since each element in the mesh could accept a different density, the optimization problems involve a large number of variables.

1.2 Design Variable Approaches

TO was introduce in 1988 by the seminal paper by Bendse and Kikuchi [1], where the homogenization approach proposed the utilization of periodically distributed small holes in a given homogeneous isotropic material. Since then, several approaches to tackle TO have been proposed.

Density Approach

This approach was suggested by Zhou and Rozvany [2], and Mlejnek [3]. Commonly known as SIMP (Solid Isotropic Material with Penalization). SIMP is the most popular topology optimization method, with several industrial applications. ([4], [5], [6], [7]). The design variable correspond to the density of the finite element (FE) which conforms the discretized design domain. The density can take any

value between 0, representing void, to 1, representing the completely solid material. The final solution should only contain zeros or ones, to represent the elements where no material is assigned and the elements with materials. Even when one is looking for a binary design, allowing the design variable to assume intermediate continuous values helps to reach convergence and relax the optimization problem. The design variable is related to the properties of the element (e.g. mechanical, thermal,...) by an interpolation function. The density approach will be expanded in this section.

Level Set Methods (LSM)

This is a more recent method introduced by Osher and Sethian [8] [9], and implemented for TO problems by Allaire, and Wang [10] [11]. This approach draws on a scalar function called Set Function which can present positive and negative values. The boundaries of the design correspond to the zero level of the Set Function. This approach also relies on FEA, but since the design is delimited by the boundary, no intermediate densities are present. The design is updated modifying the Level Set Function instead of directly modifying the boundary. The Level Set Function is commonly updated using the Hamilton-Jacobi equations, which includes a speed function and the sensitivity of moving the interface on a certain direction.

Phase Field

This approach is based on the Allen-Cahn equations, which model phase separation processes. A functional called Diffuse Interface represents the boundary of different phases, e.g. solid-void. The Diffuse Interface includes an interpolation function and the gradient norm of the density. The update of the phase field functions seeks for the direction in which the free energy function is minimized, so the resulted topologies are biased to topologies with minimal interfaces and curvature [12]. The design variables are the elemental densities, so intermediate densities are possible.

Topological Derivative

This method was proposed by Eschenauer et al [13] under the name Bubble method. The method incorporates holes (void) in the design domain and seeks for the optimal distribution of the available holes that minimizes the objective function. A sensitivity analysis is performed to predict the influence of introducing a hole on a specific FE.

Global approximation techniques

The physical model is replaced by a Response Surface Method (RSM) generated from sampling points in the design space. Therefore, there is no need of an explicit expression to relate the design variables with the response field. Among the advantages are lower computational cost, filtering of numerical noise, and insight on the entire design space. However, the minimum relies on the sampling quality.

1.3 Optimizers or updating schemes

The optimization algorithm updates the design variables after each iteration. This update is aimed at finding the minimum of the objective function. Several updating rules have been proposed for each optimization approach. Specifically, density based approaches can be solved by mathematical programming or heuristic methods. Examples of mathematical programming approaches are: Sequential Lineal Programming (SLP), Sequential Quadratic Programming (SQP), Convex Linearization method (CONLIN) [14], Method of Moving Asymptotes (MMA) [15], Optimality Criteria (OC) method. Heuristic methods to update the design variable are: Evolutionary Structural Optimization (ESO/BESO) [16], and Hybrid Cellular Automation (HCA) method [17] [18].

OC was popularized for the solution of minimum compliance problems [19] due to its efficiency. OC method can be seen as a special case of the explicit convex approx-

imation method. The gradient of the compliance can be linearized, this expression leads toward a convex problem that can be solved using the Lagrangian Duality. The updating rule obtained after solving the Lagrangian Duality shows that the minimum of the function corresponds to the design where the energy per volume (specific strain energy) is constant for every FE [20].

HCA is an algorithm inspired by bone regeneration that uses the Strain Energy Density failure criterion. HCA has been implemented for topology optimization problems [18]. For this application, the algorithm aims to equalized the Strain Energy Density (SED) for all the elements on the mesh by setting a target value called Set Point. In this case, the updating scheme is heuristic and is performed by a control system. The present work explores the capability of HCA to be implemented in multi-material optimization problems in which, the method is presented in detail further in this chapter.

1.4 Numerical Instabilities

TO seeks for the optimal topology of a component. The optimization problem is solved using FEA, numerical methods and/or approximations functions. The solution to the optimization problem is achieved over a series of iterations until a convergence criterion is met. However, the iterative process is known to present numerical instabilities [21] that difficult the convergence of the problem.

Non-existence

The 0-1 TO problem lacks solutions. The reason is that the optimization problem is ill-posed and lacks delimitation of the set of feasible designs. As explained by [21], in a structural optimization problem, the introduction of more holes maintaining the volume of the design will benefit the efficiency of the response (objective function).

Local Minima

In the case the optimization problem is a nonconvex problem the solution may lead to a local minimum. In this case, the final solution will highly depend on the starting point or initial design.

Checker board solutions

This problem consists of alternating solid and void elements on the optimization solutions in which the final design is not a continuous structure. To avoid this problem several solutions are proposed, still filtering is the most common practice. Sigmund suggested in 1994 [22] to use low pass filter techniques from image processing. The response or sensitivity of the response for each FE depends on a weighted average over the element's response and its nearest neighbors.

Mesh dependency

TO problems present different solutions according to the mesh size of the FE. This follows from the ill-possessing of the optimization problem whereas the number of finite element increases, finer structures will grow in the design.

1.5 Density Approach

The density approach takes as design variables for the optimization problem the density of the FE and relates the design variable to the material properties using a continuous variable formulation. The density approach is an artificial way of reducing complexity and promoting convergence of the optimization problem. Intermediate densities are penalized so the function favors 0 and 1 designs. The first density approach formulation was proposed by Zhou and Rozvany [2], and Mlejnek [3]. This interpolation is known as SIMP (Solid Isotropic Material with Penalization). Later,

Stolpe and Svanberg [23] proposed the RAMP (Rational Approximation of Material Properties) interpolation.

$$\begin{aligned} \text{General Inteprolation:} E(x_i) &= g(x_i)E_0 \\ \text{SIMP:} E(x_i) &= x_i^p E_0 \\ \text{RAMP:} E(x_i) &= x_i/(1+p(1-x_i))E_0 \end{aligned} \tag{1.2}$$

Where, E is the effective Elasticity Modulus, x is the density of the i-th finite element, p is the penalization, and E_0 is the Elasticity Modulus of the solid material. For values of $p > 1$ the interpolation function inhibits intermediate densities in the solution. The penalization factor should be carefully selected since it affects the convergence of the problem. Note that for high values of p the variable update may be abrupt which leads to an early convergence. Otherwise, if the value of p is smaller e.g. 1, the design may contain a considerable amount of intermediate densities. Continuation approaches vary the value of the power p along the optimization to promote the exploration, it starts with p=2 and gradually increases the value of p on every iteration of the optimization process.

Since the different formulations of density approach are continuous and easy to derive, the optimization problem can be solved by gradient based methods like Optimality Criteria (OC) or The Method of Moving Asymptotes (MMA).

1.6 Hybrid Cellular Automaton Algorithm (HCA) [18]

HCA is a method based on the Strain Energy Density failure criterion that has been previously implemented in topology optimization problems [18]. HCA is a biologically inspired algorithm that mimics the process of structural adaptation of bones. The algorithm abstracts the biological behavior applying the paradigm of Cellular Automaton (CA) used by first time to describe the operation of the heart muscles [24] [25].

CA discretizes a complex problem into a set of local problems. The space to be studied is divided into a regular grid of cells. At the beginning of the simulation each cell has an assigned state. Throughout the time (iterations), the state of the cells is updated based on a generalized rule that works locally as it depends on the previous state of each cell and its closest neighbors. For every cell, the evolution is a function of a weighted sum of the response of the cell of interest and its neighbors. By considering the influence of neighboring cells, it is possible to model the problem as a system in which the discrete parts are mutually affected.

The definition of the neighborhood can be done in different ways, Figure 1.1 shows the most common types of neighborhoods. For small neighborhoods, the state and the updating of each cell acquired independence. Contrarily, a large neighborhood distributes the states of the cells obtaining an update with less abrupt changes among the cells. The grid should be extended on the boundaries to allow the boundary cells to use the same update rule, Figure 1.2 presents some types of boundary conditions. The states of the boundary can be fixed to a specific value (a), adiabatic (b), reflecting (c) or periodic as if the design domain would be wrapped (d). In TO applications, the extended boundary cells are fixed to a state of zero to avoid its influence in the design domain.

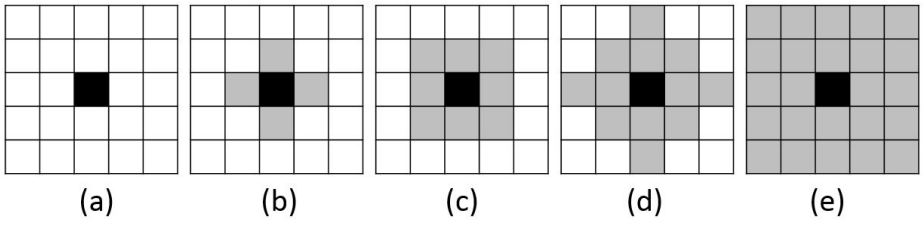

Fig. 1.1. Two dimensional neighborhoods for CA. (a)Empty (b)Von Neumann (c)Moore (d)Extended

The utilization of CA to solve shape optimization structures was presented by [26] taking the Young Modulus of each cell as the design variable and solving the response of the stress field using FEA. Kita and Toyoda [27] implemented the CA to solve TO

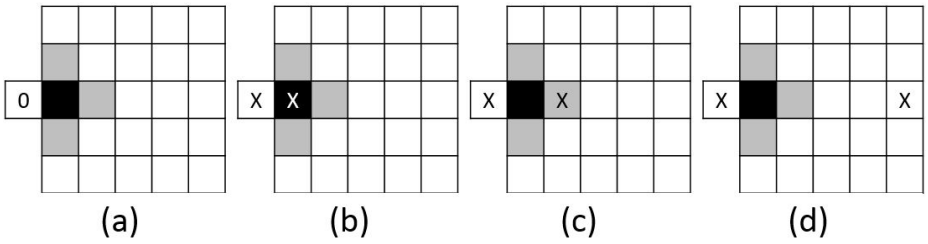

Fig. 1.2. Two dimensional boundary conditions for CA. (a) Fixed (b) Adiabatic (c) Reflecting (d) Periodic.

problems. In this work, the design variable was the thickness of each cell. The problem was formulated as a multi-objective optimization problem to minimize weight and the deviation between the yield stress and the Von Misses. However, this algorithm presents slow convergence and a high number of intermediate densities.

The Hybrid Cellular Automaton (HCA) [17] [18] as implemented for TO problems, is a density based approach with a non-gradient based updating scheme. It uses the CA paradigm in conjunction with FEA to calculate the response of the cells to the mechanical stimuli. The optimization problem solved by HCA algorithm is given by:

$$\begin{aligned} \underset{x}{\text{minimize}} \quad & |\bar{S}_i(x_i) - S^*(t)| \\ \text{subject to} \quad & \frac{\sum_{i=1}^{nele} x_i}{nele} \leq M_f \\ & 0 \leq x_i \leq 1 \end{aligned} \tag{1.3}$$

The design variable x is the density of each cell. HCA has been previously tested with linear interpolation and penalized interpolation function (SIMP), to relate the design variables with the mechanical properties of the FE. The objective function proposed corresponds to achieve a target value of strain energy density (SED) of the finite elements called Set Point (SP*). Finally, the update rule corresponds to a local control strategy that compares the response of the cells to a target value

of SED^*. The control rules that have been tested for this algorithm include two-position, proportional, proportional-derivative, proportional-derivative-integral, and radio technique.

The state of a cell consists of the design variable x_i (e.g. density), and the response or field variables (e.g. SED). As mentioned, the design variables are related to the properties, and therefore to the response by the interpolation function (e.g. SIMP). The optimization algorithm has two iterative loops. The outer loop monitors the convergence of the optimization design, and the inner loop checks the fulfillment of the constraints, e.g. volume constraint. The algorithm for HCA TO is shown below in 1. The response S is a function of the design variable x at each iteration t, as S(x(t),t). However, it has been omitted in the following pseudo-code for simplification.

Result: final design

$S^*(0)$ calculation of Set Point

$x(0)$ initial design

while *convergence has not been met* **do**

  $S(t)$ structural analysis FEA

  $\bar{S}(t) = f(S(t), S_N(t))$ filtered response

  while *volume constraint has not been met* **do**

    $S^*(t+1) = f(S^*(t), volfrac)$

    $e(t) = f(\bar{S}(t) - S^*(t))$

    $x(t+1) = f(x(t), e(t))$

  end

end

Algorithm 1: HCA algorithm

Once the design domain, boundary and loading conditions are defined, the algorithm calculates the value of a Set Point (SP) which corresponds to the reference performance that will drive the optimization process. Arbitrarily, the set point is

chosen as the average of the SED of all the elements in the mesh when the design domain is completely solid (arrangement of ones). In this way, the algorithm will attempt to even the SED along the mesh, and bring this value as close as possible to the SP. The optimization starts with an initial design for all the elements. The response (SED) for the initial design is computed using FEA. As follows, the response is averaged with the response of the cells that belong to the neighborhood:

$$\bar{S}_i(t) = \frac{S_i(t) + \sum_{n \in N(i)} S_n(t)}{N + 1} \tag{1.4}$$

Where, $\bar{S}_i(t)$ is the "filtered" response of the i-th element at the t-th iteration, $S_i(t)$ is the response obtained from the FEA, N refers to the neighborhood of the i-th element, and the denominator N corresponds to the total number of neighbors in the neighborhood.

This expression is the analog to the low pass filter used in SIMP applications, where a radius of filtering is applied. Filtering techniques are applied to the sensitivity of the objective function, whereas HCA softens the response of the design. Using the averaged response, the error with respect to previous iterations is calculated, and the local update rule is applied to update the design variables. The following are the different available updating rules:

Two Position:

$$x_i(t+1) = x_i(t) + c_T sgn(\bar{e}_i(t))$$

Proportional:

$$x_i(t+1) = x_i(t) + c_P \bar{e}_i(t)$$

Proportional Integral:

$$x_i(t+1) = x_i(t) + c_P \bar{e}_i(t) + c_I(\bar{e}_i(t) + \bar{e}_i(t-1)) \tag{1.5}$$

Proportional Integral Derivative:

$$x_i(t+1) = x_i(t) + c_P \bar{e}_i(t) + c_I(\bar{e}_i(t) + \bar{e}_i(t-1)) \quad + c_D(\bar{e}_i(t) - \bar{e}_i(t-1))$$

Ratio Technique:

$$x_i(t+1) = x_i(t) + (\frac{S_i^*(t)}{S_i(t)})^{\frac{1}{p-1}}$$

Where $x_i(t)$ corresponds to the i-th design variable at the t-th iteration. Analogously, $x_i(t+1)$ is the updated variable for the next iteration. c_T, c_P, c_I, and c_D are the control coefficients, sgn is a signal function, and $\bar{e}_i(k)$ is the effective signal error. The signal error is defined as the difference between the elemental response and the target SP. The control rules aims to minimize this error.

$$e_i(t) = S_i(t) - S_i^*(t) \tag{1.6}$$

Then, the effective error signal is defined for the cell and its neighborhood N as:

$$\bar{e_i}(t) = \frac{e_i^{(t)} + \sum_{n=1}^{N} e_n(t)}{N+1} \tag{1.7}$$

For the Two Position Control, the signal function is given by:

$$sgn(e_i\bar{(}k)) = \begin{cases} +1.0, & e_i\bar{(}t) > 0 \\ 0.0, & e_i\bar{(}t) + 0 \\ -1.0, & e_i\bar{(}t) \leq 0 \end{cases} \tag{1.8}$$

For the inner loop, the volume constraint should be less than an admissible tolerance. If the volume fraction is above the constraint, the set point SP is modified proportionally to the ratio between the actual volume fraction and the target volume fraction.

$$SP^*(t+1) = SP^*(t)\frac{M_f(t)}{M_f^*} \tag{1.9}$$

Where, SP^* is the Set Point, t is the iterator, M_f^* is the mass fraction target i.e. design constraint, and M_f is the actual mass fraction. The mass fraction is calculated as the average mass of the design domain since all the FE have the same volume (dimensions).

$$M_f(t) = \frac{\sum_{i=1}^{nele} x_i(t)}{nele} \tag{1.10}$$

Where nele refers to the number of elements. If the volume constraint is satisfied, the inner loop breaks. Once the design meets the volume constraints, a new iteration begins and the response (SED) of the new design is computed. After each outer loop, the convergence of the model is checked, and the optimization stops when the convergence criterion is met.

The convergence criterion is met when the change in the mass of two consecutive iterations is less than a tolerance value. The mass change of two iterations is used to avoid premature convergence [18].

$$\Delta M(t) = \sum_{i=1}^{nele} |x_i(t) - x_i(t)| \tag{1.11}$$

With, ΔM the change in the mass for the t-th iteration, nele is the number of elements in the design space, and $x_i(t)$ is the density of the i-th element on the t-th iteration.

The control rules used to locally update the design variable, the power p, and the initial design have a major influence in the convergence and the solution of the optimization. The SP chosen also influences the final solution of the optimization. The final response is proportional to the value of the SP, and the final volume fraction is inversely proportional to the SP. However, the algorithm doesn't show mesh dependency with the refinement of the mesh; only higher resolution and computational time was observed [17].

1.7 Objective

The objective of the present work is to explore and implement the HCA algorithm as a control system for multi-material topology optimization. HCA has proven to be an efficient algorithm in binary topological optimization with the great advantage of not requiring sensitivity information. The expansion of the HCA algorithm for crash-worthiness applications, and its adoption by commercially available software, demonstrate the versatility of control systems in optimization problems.

The work is organized as follows: The second chapter starts with a recapitulation

of existing approaches for multi-material topology optimization. Two recently proposed algorithms based on the density approach are detailed. These two algorithms are tested to highlight their advantages and disadvantages. Subsequently, the work comments on the optimization for dynamic loads and the implementation of HCA for crash-worthiness applications. The next chapter introduces the expansion of the proposed HCA algorithm to solve multi-material problems. Two-dimensional numeric examples are shown for static and dynamic loading problems.

2. MULTI MATERIAL TOPOLOGY OPTIMIZATION

The conception of TO was a revolutionary contribution since made possible to automatize the iterative design process, allow the analysis of complex problems, and take advantage of the emerging manufacturing technologies that can handle a bigger complexity in terms of shapes and resolution. Since TO seeks the optimal material distribution, the idea was initially focused on obtaining a binary design of void or solid material. However, the field has been increasing even more the complexity of the design as implementing multi-scale topology optimization and multi material topology optimization, pointing toward more efficient structures in terms of material utilization, manufacturing cost and performance (mechanical, electrical, thermal, etc.).

Multi Material Topology Optimization (MMTO) expands the idea of the TO, where the topology of the design matters in addition to the distribution of different materials. Several materials or phases could be considered to integrate into the same model because of a trade-off between performance properties (e.g. elasticity modulus, yield strength, heat conduction coefficient, etc.) and non-directly related performance properties (e.g. time of production, cost, weight, degradation, etc.).

2.1 Current approaches

There are several proposals for MMTO with different TO approaches. In 1997, Sigmund and Torquato [28] solved the problem by implementing homogenization and expanding the SIMP interpolation for three phase materials. This density based approach was later implemented in composite material optimization, and is referred to as Discrete Material Optimization (DMO) [29], [30], [31]. In this method, the

interpolation function that relates the material properties and the design variables is expressed as an artificial mixture of the three (or more) phases, complying with the upper and lower Hashin-Shtrikhman bounds. The optimization was solved using Linear Programming Algorithms (LP). The results converged to optimal and organic shapes, however, the computational time required to solve the problem was considerably high even for coarse meshes. Using a similar approach to that of Sigmund and Torquato [28], Tavakoli and Mohseni [12] proposed a solution that works with the optimization of all the possible combinations of the considered phases. Recently, Zuo and Saitou [32] presented a piece-wise interpolation function approach for the optimization with multiple materials. These last two works will be described in detail in the next section because they were used as a benchmark for the multi-material expansion of the HCA algorithm.

In the Level Set approach, a possible solution for multi-material optimization problems is defining a level set function for each material considered; in this way, the number of level set functions required is equal to the number of materials. However, overlaps among the different phases and subsequently, intermediate densities, are unavoidable. Wang and Wang [33] proposed a method referred to as Color level set which appeals to set theory. In this case, the number of m set functions required decreases, as for a design with $n = 2^m$ materials, the algorithm uses $m = log2n$ level set functions. The phases are assigned to different sets according to the union or intersection of the level set functions so intermediate densities are not possible.

Zhou and Wang [34] extended the phase field approach based on the Cahn-Hillard equations for MMTO. The Cahn-Hillard model is adapted for mechanical loads and deformations. To consider several materials, the authors represent the material properties of an element as a weighted sum of the material properties of each phase, similar to the density approach. The solution is characterized by favoring the grouping of the materials which may have advantages for manufacturing proposes, however, the optimization takes thousands of iterations to converge.

Ramani [35] solved the problem with discrete variables. The method estimates the

change (pseudo sensitivity) of a failure function when an element changes to the immediately lower and higher density materials. Based on the pseudo sensitivity, the elements are ranked, and only a fraction of the elements are updated for the next iteration. Ramani used a finite-difference approximation to compute the pseudo sensitivity which may be inefficient for a large number of design variables. The algorithm is solved with an evolutionary approach similarly to [13].

It is worth mentioning that most of the work done to date, including the present study, is in an exploratory phase. In the proposed methods for structural applications, the variety of materials is modeled only through the magnitude of the isotropic modulus of elasticity. Other mechanical properties have been little used and assumed equal for all the materials (e.g. Poisson ratio). Also, perfect bonding between the phases is assumed. The modeling of the union mechanisms between phases, and including these mechanisms within the considerations of the optimization process, represents one of the biggest challenges in the multi-material optimization.

The following presents a detailed description of the density and gradient based MMTO proposed by [12] and [32]. This algorithm will be compared against the performance of the modified HCA MMTO algorithm.

2.2 Alternating Active Phase Algorithm [12]

Tavakoli and Mohseni [12] proposed a density and gradient based MMTO that divides the optimization problem into binary-phase optimization sub-problems. In every iteration, the binary-phase optimization is performed for all the possible combinations of the phases, so the algorithm performs $n(n-1)/2$ optimization in every iteration, where n represents the number of materials considered. As it is possible to observe, the number of function calls increases exponentially as the number of materials increases. Below is the pseudo-code for the Matlab implementation.

Result: final design

$\mathbf{x}(0)$ initial design

while *convergence has not been met* **do**

  for *all the possible combinations of two materials* **do**

    $S(t)$ structural analysis FEA

    $c(x) = f(S(t), x(t))$ compute objective function

    $dc(x) = f(S(t), x(t))$ compute sensitivity of objective function

    $\bar{dc}(c) = f(dc(x), dc_N(x)$ filtered sensitivity

    while *volume constraint has not been met* **do**

      $\mathbf{x}(t+1) = f(\mathbf{x}(t), \bar{dc}(t))$

    end

  end

end

Algorithm 2: Active Phase algorithm

The interpolation function used to relate the material properties with the design variables corresponds to a weighted sum of the individual contributions of all the materials to the element. The author used the expression previously proposed by [2]:

$$E(x_i) = \sum_{m=1}^{M} x_{i,m}^{p} E_m \tag{2.1}$$

Where x_i is the density of the element (design variable), $E(\mathbf{x})$ is the property of the element (Young Modulus), M is the number of materials been considered, p is the penalization factor, $x_{i,m}$ is the density or weight that indicates the influence of a the m-th material in the i-th element, and E_m is the Young Modulus of the m-th material.

At this point, the author makes a clarification. The interpolation equation used may result in non-physical data, as in some singularity cases the Hashin-Shtrikman bounds could be violated [30]. However, to find the Hashin-Shtrikman bounds for an arbitrary

number of phases is complex and may not be possible in some cases [36].

During the binary-phase optimization, the remaining phases are deactivated. The algorithm uses the matrix of x densities as design variables. In this matrix, the rows correspond to the elements in the design space, and the columns correspond to the different materials available. The sum of the density values on each row (same element) must add 1, that is, the densities represent the contribution or weight of each material in the performance of the element. When a binary-phase optimization is performed, only the densities of the two materials in consideration are modified by the optimizer.

These binary-phase optimization subproblems are solved using the traditional density based topology optimization. The author implemented the algorithm on a 115 line code in Matlab. As implied previously, the algorithm works with FEA to obtain the response of the design and the OC criterion was used to solve the optimization. A filter is applied to the objective function sensitivity to avoid checker boarding. The code was implemented to solve the minimum compliance problem, and a volume constraint was defined for each material.

2.3 Ordered SIMP Algorithm [32]

The second algorithm of interest was presented by Zuo and Saitou [32]. This algorithm is also a density based approach solved with gradient information, as does the OC method. However, unlike most of the density based MMTO algorithms proposed that used the extended SIMP interpolation, Zuo and Saitou proposed a piece-wise interpolation equation. The following presents the pseudo-code for this proposal:

Result: final design

$x(0)$ initial design

while *convergence has not been met* **do**

  $\bar{E}(x), \bar{P}(x)$ interpolated proprieties

  $S(t)$ structural analysis FEA

  $c(x) = f(S(t), x(t))$ compute objective function

  $dc(x) = f(S(t), x(t))$ compute sensitivity of objective function

  $\bar{dc}(c) = f(dc(x), dc_N(x)$ filtered sensitivity

  while *volume constraint has not been met* **do**

    $x(t+1) = f(x(t), dc(t))$

  end

end

Algorithm 3: Ordered SIMP algorithm

The algorithm works with three vectors of material properties for each phase under consideration: physical density vector, elasticity vector, and cost vector. The vectors are normalized, i.e. each vector has values from 0 to 1. The physical density vector drives the optimization process and is sorted in ascending order. The other two vectors are ordered consistently so that each material has its properties in the same position of each vector.

The piece-wise interpolation equation to relate material density (x) with the elasticity modulus (E) is obtained with the scaling coefficient A_E and the translation coefficient B_E as:

$$\begin{aligned} E(x_i) &= A_E x_i^p + B_E \quad if \quad \rho_m < x_i \leq \rho_{m+1} \\ &\text{with,} \\ A_E &= \frac{E_m - E_{m+1}}{\rho_m^p - \rho_{m+1}^p} \\ B_E &= E_m - A_E \rho_m^p \end{aligned} \tag{2.2}$$

Where the subscripts m and m+1 refer to the position of the material properties in the ordered vector.The design variable x corresponds to the density of the element, ρ represent the density, and E the Elasticity modulus; the last two are properties of the desired materials. A second interpolation equation is used to relate the density of the material with the cost property. To reflect the preference of the designer for a lower cost, the penalization factor is substituted by $1/p$. Here, the scaling coefficient is given by AC and the translation coefficient is given by BC in:

$$\begin{aligned} C(x_i) &= A_C x_i^{1/p} + B_C \quad if \quad \rho_m < x_i \leq \rho_{m+1} \\ &\text{with,} \\ A_C &= \frac{C_m - C_{m+1}}{\rho_m^{1/p} - \rho_{m+1}^{1/p}} \\ B_C &= C_m - A_C \rho_m^{1/p} \end{aligned} \tag{2.3}$$

Where the subscripts m and m+1 refer to the position of the material properties in the ordered vector. Figure 2.1 illustrates both interpolation curves. In this Figure both equations are monotonically increasing; however, this may not be always the case since usually a trade-off between properties is present in optimization problems. As summarized in Figure 2.2, the authors considered all the possible cases in the interpolation equations. In this image, the case (d), one material is strictly dominated for both properties so the material should be deleted and not considered in the optimization problem.

Since Ordered SIMP works with a piece-wise equation delimited for a higher density material and a lower density material, the Hassin-Shtrikman bounds were calculated and the author concluded that the interpolation equations satisfy the bounds. The Ordered SIMP algorithm was implemented to minimize the compliance under cost and volume constraint. If desired, one constraint could be turn off by simply using a constraint equal to 1.The algorithm applies a sensitive filter to overcome the numerical instabilities known for TO.

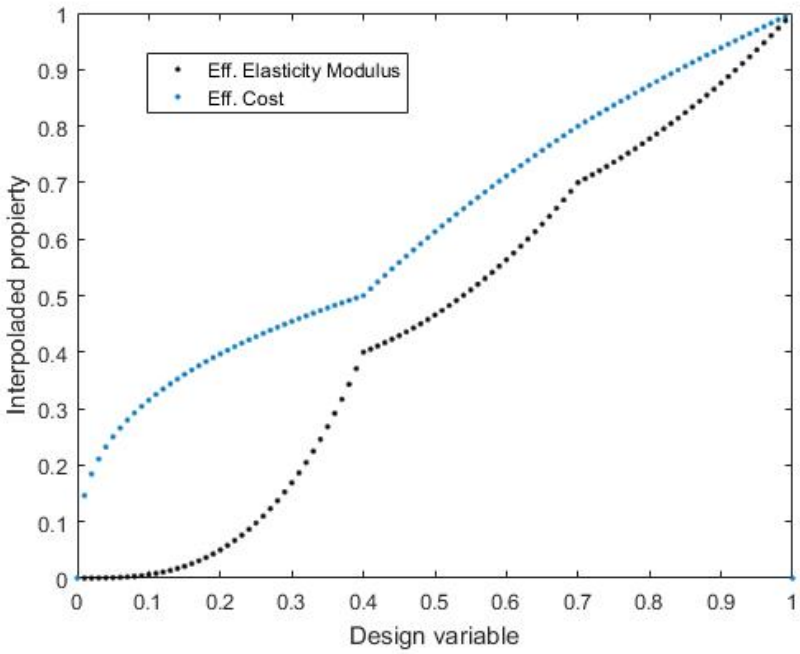

Fig. 2.1. Interpolation curves for modulus of elasticity and cost for a monotonic three phases optimization.

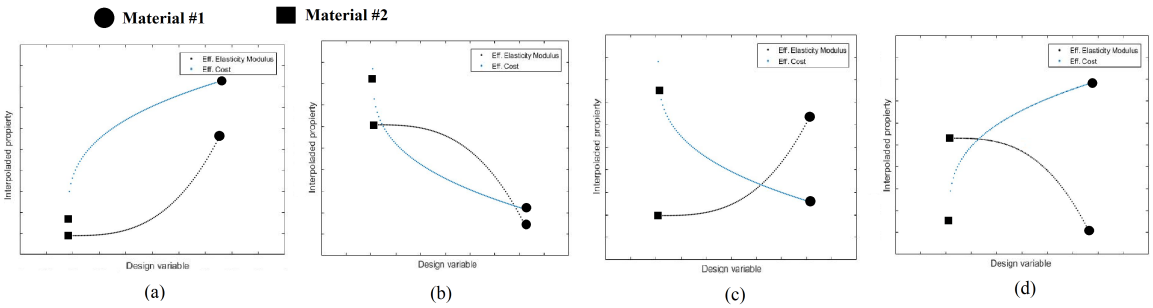

Fig. 2.2. Possible cases of interpolation function for two materials.

3. CRASHWORTHINESS TOPOLOGY OPTIMIZATION

Crashworthiness is the ability of an object to resist a collision. Most efforts in crashworthiness have applications in vehicle safety, which focuses on occupant protection to reduce the number of fatal and serious injuries in case of collision. Crashworthiness design emerged during the decade of the 50s for the aerospace industry and started to develop in the decade of the 60s for the automotive industry. The main considerations are to design structures with the ability to deform plastically in order to absorb part of the kinetic energy of the collision, to minimize the intrusions in the areas occupied by the passenger, and to maintain an acceptable deceleration load. As it is possible to notice, the design for crashworthiness structures is complex because of the compromise of its requirements between stiffness and deformability.

3.1 Current approaches

Topology optimization techniques have been widely developed for isotropic, linear elastic and static problems. Models of crashworthiness events have a higher complexity with nonlinear interactions like material nonlinearities, geometry, and transient nature of boundary conditions [37]. Most of the TO approaches use sensitivities to solve the optimization problems; in the case of linear static problems, the sensitivities are inexpensive to obtain; however, computing sensitivities for dynamic problems is expensive and non-practical. The development of algorithms for crashworthiness TO needs to be further explored.

Following is presented a brief introduction to the development of crashworthiness TO approaches. Fang et al [38] published a detailed state of the art on crashworthiness TO. Mayer et al. [39] addressed the first TO problem for crashworthiness in 1996

implementing the homogenization technique using the internal energy as objective function. Pedersen [40] implemented TO for 2D frame structures. In his work, the objective was to minimize the error between the acceleration of the nodes and a prescribed acceleration. The optimization was solved using sensitivity information, which increases the computational cost of the solution. Besides, no contact information was included in the design. Soto [41] purposed an approach where a structure to efficiently absorbed energy, would distribute the plastic deformation. For this, the design domain had to achieve a prescribed distribution of plastic deformation. This was a heuristic method, so no sensitivity information was required.
Other approaches have opted for simplifying dynamic nonlinear problem through equivalent static and/or linear counterpart. There are two main approaches.

• Equivalent Static Loads (ESL): This approach was extended by Park [42] for topology optimization in 2011. This approach divides the optimization problem in two sub-problems: nonlinear simulation and linear optimization. The respond field is computed using nonlinear analysis. Following, the ESL that produce an approximated response field are calculated. Finally, the ESL are used as external loads for a linear static topology optimization design. The new design is tested again under nonlinear conditions, the optimization continuous for several iterations until convergence is reached. There is limited literature regarding crashworthiness topology optimization using ESL. The main concern to be addressed in future research is whether the equivalent static loads represent the field response, considering that during a crash event the stiffness of the structure changes [43].

• Inertia Relief Method (IRM): IRM is used in the analysis of unconstrained structures, e.g. aircraft and spacecraft. Static analysis cannot be used to solve unconstrained structures because of the singularity of the stiffness matrix. IRM assumes a static equilibrium state between the external forces and the inertia forces of rigid body acceleration produced during the unconstrained motion. The external load is

calculated and is used to later perform the FEA. IRM has gained attention as a practical engineering approach for crashworthiness TO [43]. Chuang and Yang [43] performed a crashworthiness optimization implementing IRM using Optistruct software. The problem formulation intended to minimize compliance for a frontal impact under mass constraint; the design converged in 55 iterations.

3.2 HCA for Crashworthiness Topology Optimization [37]

HCA is an algorithm that has been implemented to solve density based TO problems, with a non-gradient based updating scheme. Since the control feed does not require sensitivity information, HCA offers flexibility on the setting of the optimization problem, in terms of objective function and constraints. Patel et al. [44] proposed an implementation of HCA to perform crashworthiness TO in three-dimensional designs. The objective is to obtain uniform strain energy density (SED) while constraining the mass. The pseudocode of the algorithm is shown in the algorithm 4.

Result: final design

$S^*(t)$ calculation of Set Point

$x(0)$ initial design

while *convergence has not been met* **do**

  $S(t)$ structural analysis FEA

  $\bar{S}(t) = f(S(t), S_N(t))$ filtered response

  $\bar{S_h}(t) = f(\bar{S}(t), \bar{S}(t-1), \bar{S}(t-2), \bar{S}(t-3))$ response memory

  while *volume constraint has not been met* **do**

    $S^*(t+1) = f(S^*(t), volfrac)$

    $e(t) = f(\bar{S_h}(t) - S^*(t))$

    $x(t+1) = f(x(t), e(t))$

  end

end

Algorithm 4: HCA algorithm for crashwrothiness

The goal in crashworthiness design is to absorb the maximum energy with an acceptable peak load, as well as minimizing the intrusions near the passenger. In this way, crashworthiness TO can be addressed as a multi-objective topology optimization, increasing, the complexity of the problem. The work by Patel et al. [44] focuses on the energy absorption of the design using the strain energy density (SED) as the objective function for the optimization problem. In ductile materials such as metals (commonly used materials in automotive applications), the energy absorption is achieved by elastic and plastic deformation and folding. The SED is defined as,

$$U = U^e + U^p = \int_0^{\varepsilon_f} \sigma : d\varepsilon \tag{3.1}$$

Where U is the total energy absorbed by the structure, U^e and U^p are the energy absorbed through elastic and plastic mechanisms, ε_f is the final strain, and σ is the stress. The SED is illustrated in Figure 3.1.

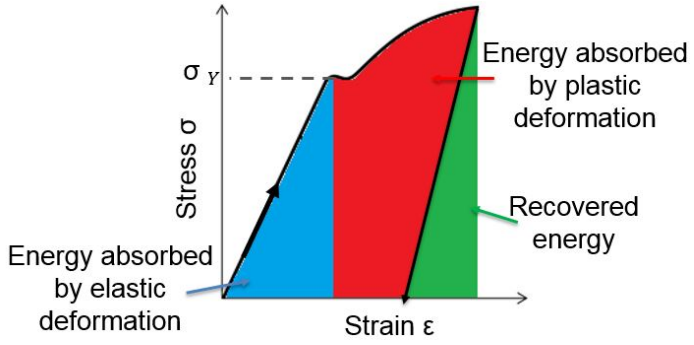

Fig. 3.1. 4 Stress-strain curve for inelastic events. The area under the curve represents the dissipated energy. [37]

SED can be maximized by maximizing the area under the curve of strain-stress. In a discretized structure, as in the case of FEA, the energy absorbed by each element can be computed from the transmitted force to each element and its corresponding displacement.

The algorithm used for crash-worthiness TO is similar to the algorithm for the linear HCA TO previously explained. As in the linear scheme of HCA, the material parametrization is performed using the density based approach with SIMP interpolation. The response of the design, in this case, SED, is obtained using a dynamic FEA, therefore the equilibrium equation is given by:

$$\mathbf{M}\ \mathbf{a}(t) + \mathbf{C}\ \mathbf{v}(t) + \mathbf{K}\ \mathbf{d}(t) = \mathbf{F}(t) - \mathbf{R}(\mathbf{d}, t) \tag{3.2}$$

Where, $\mathbf{a}(t)$, $\mathbf{v}(t)$, $\mathbf{d}(t)$, are the acceleration, velocity, and displacement; $\mathbf{M}$, $\mathbf{C}$, $\mathbf{K}$ are the mass, damping, and stiffness matrices respectively; $\mathbf{F}$ is the external force, $\mathbf{R}$ is the residual. The analysis is terminated at a specific time.

Then, the optimization problem is set as:

$$\begin{aligned} \underset{x}{\text{minimize}} \quad & |\bar{S_h}, i(x_i) - S^*(t)| \\ \text{subject to} \quad & \frac{\sum_{i=1}^{nele} x_i}{nele} \leq M_f \\ & 0 \leq x_i \leq 1 \end{aligned} \tag{3.3}$$

Where, S^* is the Set Point response, and $\bar{S_h}, i(x_i)$ correspond to the effective response of a cell, which is calculated considering the response of the neighborhood as in equation 1.4 and the history of the responses, as explained below.

To reduce the oscillations in the material distribution between iterations, the field state of each element corresponds to an exponential moving average of the SED state at the current iteration and T previous iterations [37]. This information gives memory proportional to the density of each element. Patel proposed a value of T=3. The field state is computed as:

$$S_i(t) = \frac{\sum_{j=0}^{T} w_i(t)^j U_i(t-j)}{\sum_{j=0}^{T} w_i(t)^j} \quad where \quad w_i(t) = (x_i(t) - x_{min})^2 \tag{3.4}$$

Several issues have been discovered concerning the use of the software that question the robustness of HCA for nonlinear applications; some of the main concerns are the high number of iterations required to converge, aand a non-periodic oscillatory behavior on the objective function [43] [38].

The commercial software Ls-Tasc was developed [45] based on the work by Patel et al to address nonlinear TO as a nested formulation. Ls-Tasc performs the optimization using FE, and the dynamic simulation of the design is executed in LS-DYNA. Ls-Tasc generates cards for discrete intermediate material densities; this allows a smoother transition between the continuum optimization and the discrete simulation in LS-DYNA. Initially, the same material is assigned to all the elements of the mesh. After the initiation, the input deck for LS-DYNA is overwritten according to the update of the material densities of each element at each iteration. Elements may be added or deleted in each iteration. An element is deleted if its density surpasses the lower possible bound of the density.

As the original HCA approach, the response (SED) is filtered using information of the neighborhood. A proportional control update rule is implemented as:

$$x_i(t+1) = x_i(t) + \Delta x_i(t) = x_i(t) + H\frac{\bar{S}_i(t)}{S^*(t)} \tag{3.5}$$

Where, H is a scaling factor, and the change is given by the ratio of the effective field response and the target set point S^*.

3.3 Crashworthiness Multi Material Topology Optimization

In the area of multi-material topology optimization works are developed implementing surrogate models. Liu [46] proposed a method to design graded cellular materials on a thin-walked structure. The methodology includes two optimizations and is divided into three main steps. The first stage is conventional topology optimization to minimize the compliance. The second stage is clustering the design variable using a machine learning algorithm called K-mean. Finally, the third stage results in a meta-model based optimization to maximize the internal energy absorption of the structure. The final design does not include values of intermediate densities as it selects cellular material phases from a predefined library. The computational cost of solving this algorithm a small fraction of the cost of a FEA. Liu [47] developed a generalized methodology for the MMTO design using clustering techniques. This work included numerical examples for crashworthiness of an armor plate and an S-rail frontal impact; for the former, the objective function was to minimize the penetration and the mass of the plate, in the second case, the goal was to maximize the strain energy absorption and minimize peak crushing force.

HCA promises to have applications in multi-material topology optimization for crashworthiness. Some advantages are that the control updating rule allows the flexibility to work the problem as a black box. This is specially used for complex optimization problems as dynamic loading conditions. Also, the SED as an objective function offers a great advantage in MMTO problems, since the state of the cell is a trade-off between the mechanical property (Young Modulus) and the deformation. Finally, the Ls-Tasc formulation with cards for intermediate material densities offers the flexibility to implement a multi-material interpolation approach.

4. EVALUATION OF MMTO ALGORITHMS

In this section, we analyze the performance of two algorithms proposed to perform MMTO with density based approach. The lessons learned from the comparison were implemented in the MMTO HCA algorithm. The density approach is flexible to be implemented for MMTO applications given that the interpolation function allows the existence intermediate densities that can be penalized according to the need of the designer. As mentioned before, for the scope of this project, and most of the work that has been developed for MMTO, the material phases are mainly differentiated by the elasticity modulus; other properties as Poisson ratio are considered same for all the phases.

The two algorithms chosen are the Alternating Active Phase [12], and Ordered SIMP [32]. Both algorithms have been addressed in previous sections. Both proposals were developed using the density approach and resort to OC to solve the optimization. Two numerical examples are presented: the well-known example of the Messerschmitt-Blkow-Blohm (MBB) beam, and a Body in White (BIW) structure of an automotive. The models are presented in two mesh sizes, for three material optimizations, and for different volume constraints. The Figure 5.2 shows the boundary conditions for the simulation.

The convergence of the objective function and the density distribution were monitored to compare the performance of the algorithms. In order to quantify the number of intermediate undesired densities, the following resolution error was formulated:

$$e_E = \sum_{i=1}^{nele} \left(\prod_{m=1}^{M} (E_m - E(x_i))^2 \right) \tag{4.1}$$

Where e_E is the resolution error, nele is the number of elements, M the number of considered materials, E_m the elasticity modulus of the m-th material, and $E(x_i)$ is the elasticity modulus obtained by the interpolation function for the i-th element in the mesh. The resolution error is normalized against the maximum possible value; this occurs when all the elements on the mesh are assigned the more distant density value from the values of the given material vector. The normalized error is given by:

$$e_{E,N} = \frac{\sum_{i=1}^{nele}(\prod_{m=1}^{M}(E_m - E(x_i))^2)}{nele * (\prod_{m=1}^{M}(E_m - E(x_i))^2)} \tag{4.2}$$

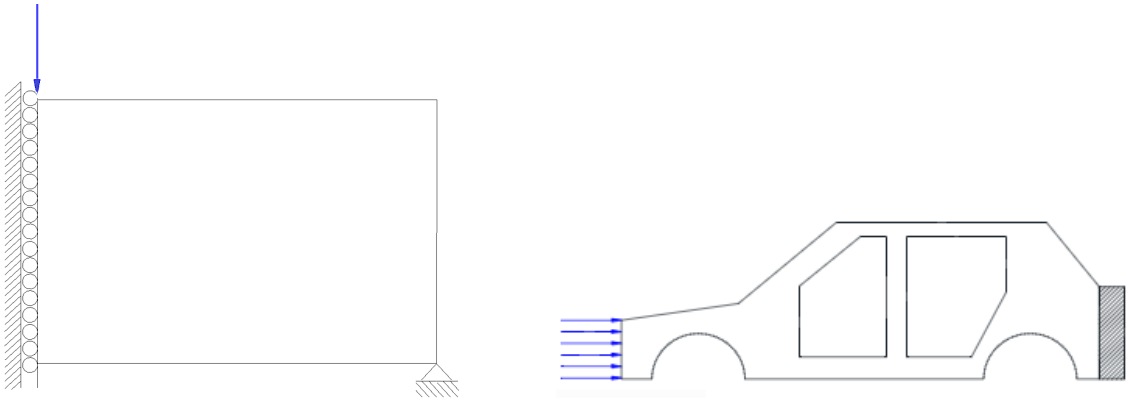

(a) MBB (b) BIW

Fig. 4.1. Simulation boundary conditions.

4.1 Alternating Active Phase

The simulation parameters are presented in table 4.1.

Table 4.1.
Active Phase Simulation Parameters

Parameter	**MBB**	**BIW**
Coarse mesh	60x20	60x20
Fine mesh	150x50	150x50
Penalization	3	3
Coarse mesh filter radius	3	3
Fine mesh filter radius	15	15
Elasticity Modulus	E=[1 0.5 1e-9]	E=[1 0.5 1e-9]
Vol Frac 0.30	volfrac=[0.15 0.15 0.7]	-
Vol Frac 0.50	volfrac=[0.25 0.25 0.5]	volfrac=[0.25 0.25 0.5]
Vol Frac 0.70	volfrac=[0.35 0.35 0.3]	volfrac=[0.35 0.35 0.3]

The algorithm has the advantage of being user-friendly and interactive in that it allows the user to decide the volume fraction of each material.A characteristic mark observed in the designs obtained in these simulations and those presented by Tavakoli and Mohseni is that of the solutions tend to group the materials. This can bring advantages in manufacturing considerations and benefit the performance of the design by having fewer interfaces.

The designs converge in an acceptable number of iterations as seen in Figure 4.3, however, the Wall-clock time to perform the iterations was significant due to the large number of function calls per iteration. The optimization time increases with respect to the number of materials. It is observed that for high values of volume fraction, a larger number of undesired intermediate densities are generated. This indicates that the value of the filter must also be modified according to the constraints.

The resolution error (Figure 4.4) shows that even after the convergence criterion

has been met, the resolution continues varying until reaching convergence after 100 iterations. The design with the intermediate volume fraction presents low resolution error, whereas the design with larger volume fraction presents an error up to 0.5 during the first iterations for the finer mesh.

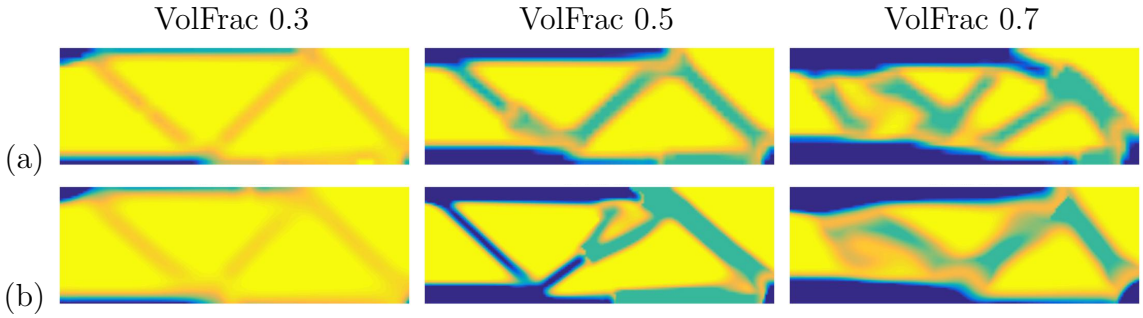

Fig. 4.2. Designs for MBB using Alternating Active Phase (a)Mesh of 60x20 (b) Mesh of 150x50.

For the BIW design (Figure 4.6)the algorithm is successful in creating a load path. The solution shows a preference to incorporate the more elastic material at the front of the vehicle and near the rear wheel. The solution show no mesh dependency. Finer meshes result in more organic designs, and the undesired intermediate densities are reduce. In general, this algorithm presents jumps in the error resolution function. The definition of materials is not established in a smooth way through the iterative process.

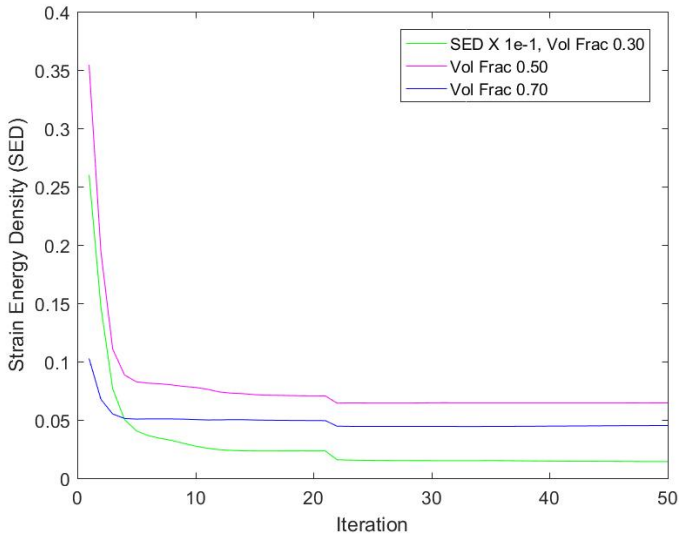

(a) Mesh of 60x20

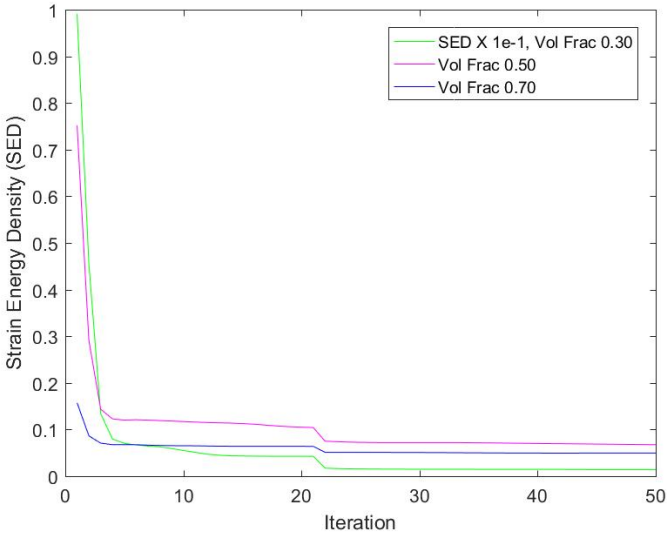

(b) Mesh of 150x50

Fig. 4.3. SED function convergence for MBB using Alternating Active Phase.

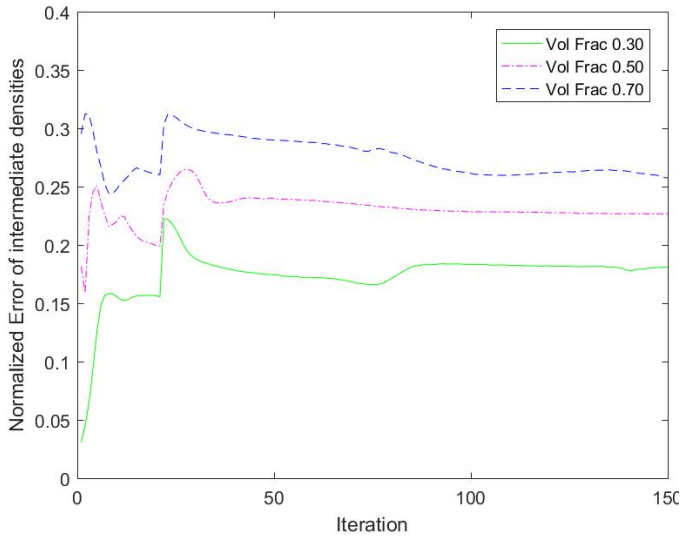

(a) Mesh of 60x20

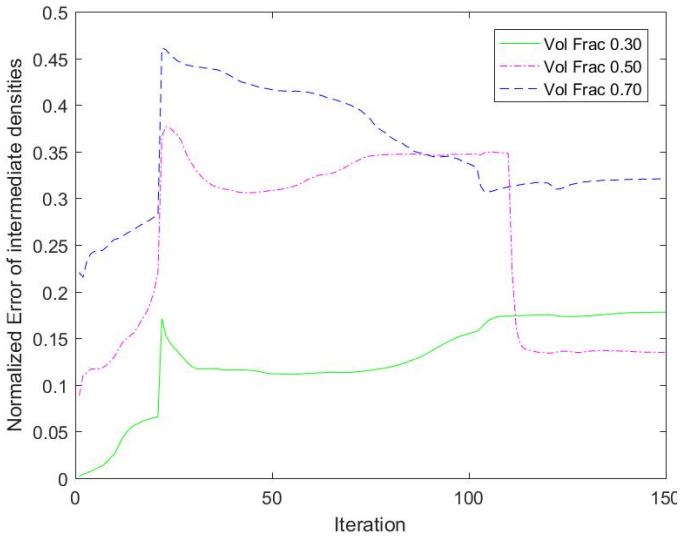

(b) Mesh of 150x50

Fig. 4.4. Normalized resolution error for MBB using Alternating Active Phase.

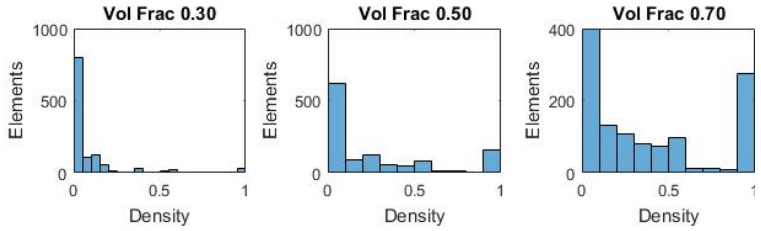

(a) Mesh of 60x20

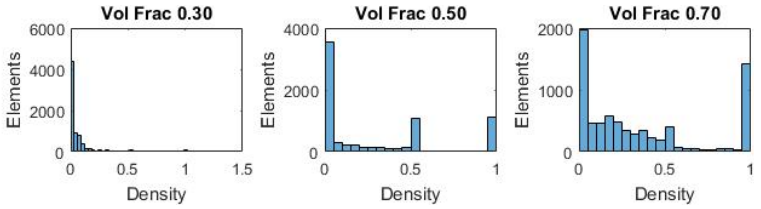

(b) Mesh of 150x50

Fig. 4.5. Density distribution for MBB using Alternating Active Phase.

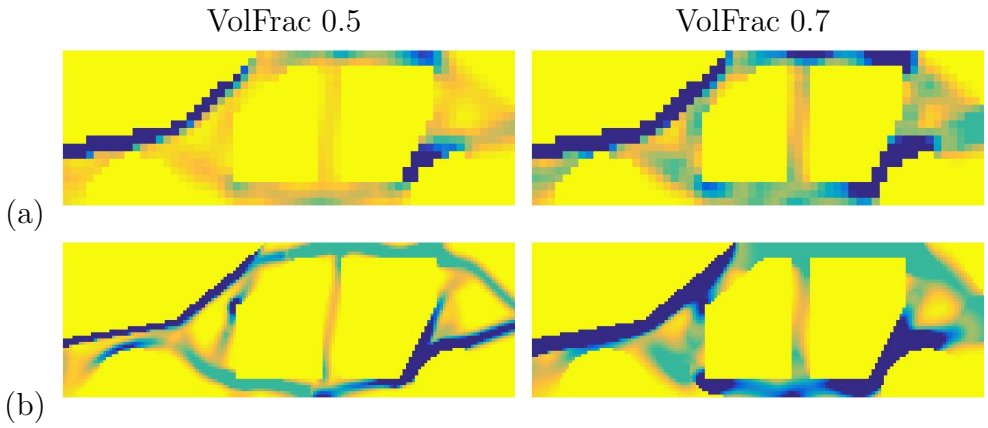

Fig. 4.6. Designs for BIW using Alternating Active Phase (a)Mesh of 60x20 (b) Mesh of 150x50.

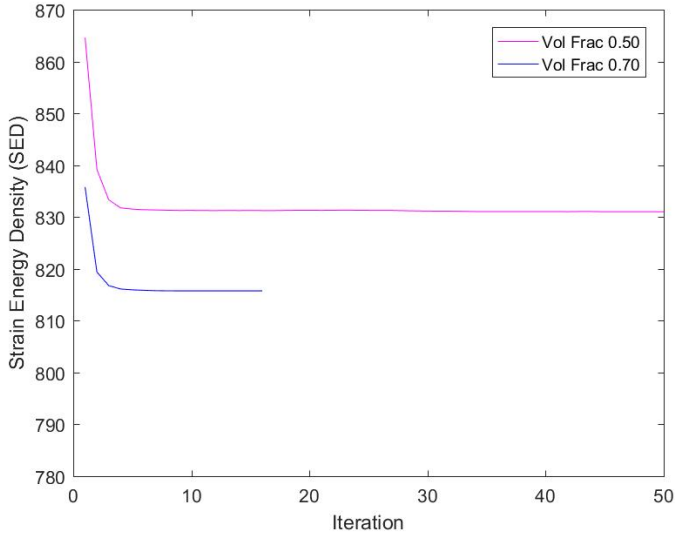

(a) Mesh of 60x20

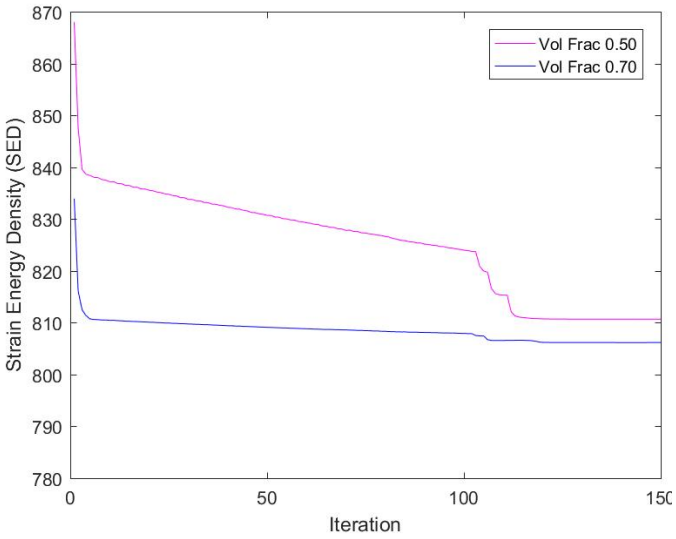

(b) Mesh of 150x50

Fig. 4.7. SED function convergence for BIW using Alternating Active Phase.

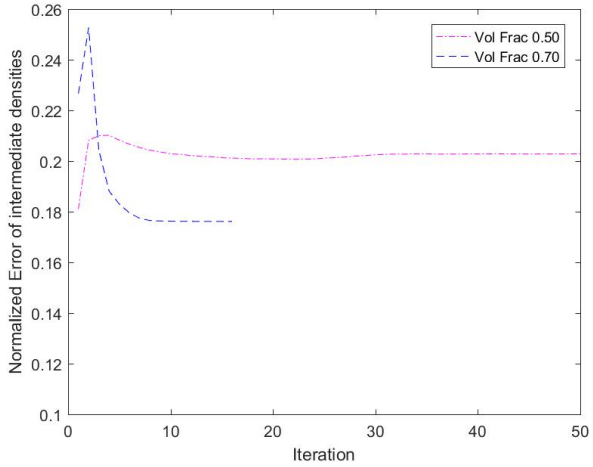

(a) Mesh of 60x20

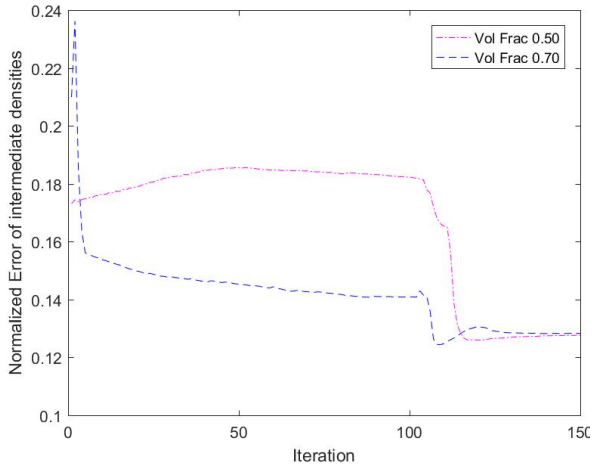

(b) Mesh of 150x50

Fig. 4.8. Normalized resolution error for BIW using Alternating Active Phase.

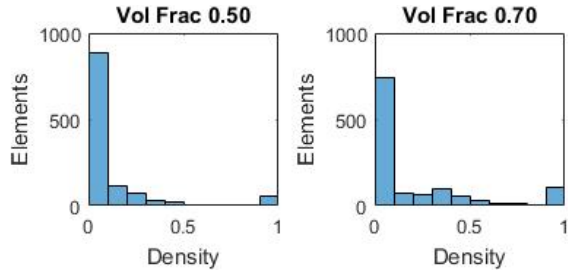

(a) Mesh of 60x20

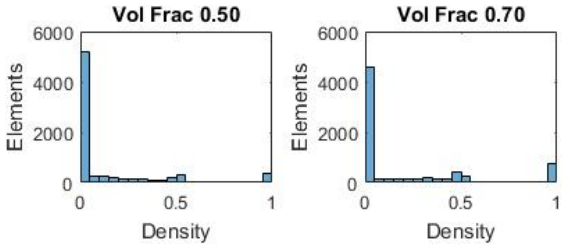

(b) Mesh of 150x50

Fig. 4.9. Density distribution for BIW using Alternating Active Phase.

Table 4.2.
Ordered SIMP Simulation Parameters

Parameter	**MBB**	**BIW**
Coarse mesh	60x20	60x20
Fine mesh	150x50	150x50
Penalization	3	4
Coarse mesh filter radius	2	3
Fine mesh filter radius	15	15
Elasticity Modulus	E=[0 0.5 1]	
Density	D=[0 0.7 1]	
Price	P=[0 0.8 1]	
Case 1	massfrac=0.3 costfrac=0.25	-
Case 2	massfrac=0.5 costfrac=0.4	massfrac=0.25 costfrac=1
Case 3	massfrac=0.7 costfrac=0.3	massfrac=0.35 costfrac=1

4.2 Ordered SIMP

The simulation parameters are presented in table 4.2.

This algorithm reduces the decision making of the user, while it determines the distribution of the materials based on a trade-off between the mass and cost constraints. However, it was verified through several simulations that the value of the property vectors (density, elasticity, and price) and restrictions; can destabilize the convergence of the solution with undesired intermediate densities. Most property and constraint configurations offer designs with large percentages of unwanted densities. The simulations presented below for the MBB and the BIW correspond to configurations that provided acceptable results for the mesh size and the established boundary conditions.

Although the solutions depend to a large extent on the properties of the materials and the loading conditions, in general the code tends to converge in less than 50 iterations

for medium-sized meshes. The wall-Clock time for this approach is considerably less than the time required through Alternating Active Phase. Since the constraint is over the mass instead of volume, the designs have a preference for using void as little as possible. The void is replaced by the following lighter material in order to improve the mechanical performance. Finally, the solutions tend to distribute the material in cores (as seen in Figure 4.10) with the stiffer material (blue) covered by the second more elastic material (light blue).

The BIW optimization was unstable through several attempted configurations. For the presented simulation (Figure 4.14), the algorithm could not define a load path. The stiffer material is concentrated at the frontal section.

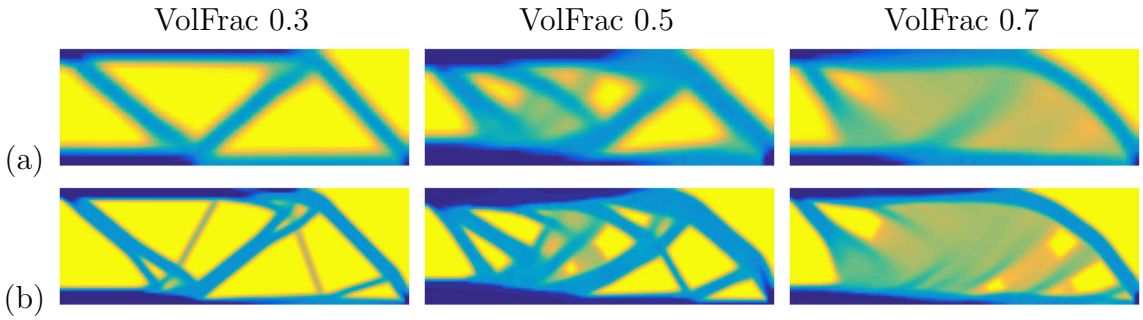

Fig. 4.10. Designs for MBB using Ordered SIMP (a)Mesh of 60x20 (b) Mesh of 150x50.

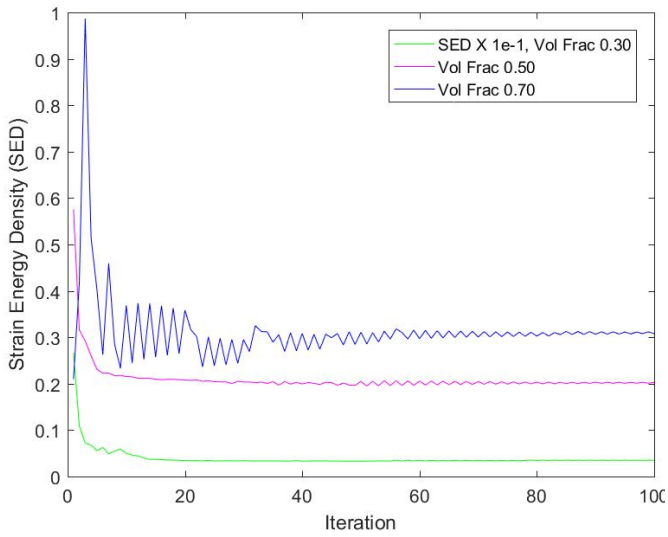

(a) Mesh of 60x20

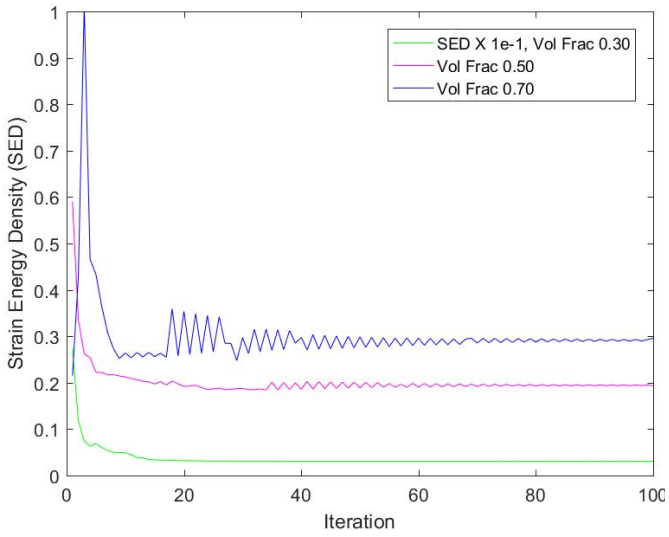

(b) Mesh of 150x50

Fig. 4.11. SED function convergence for MBB using Ordered SIMP.

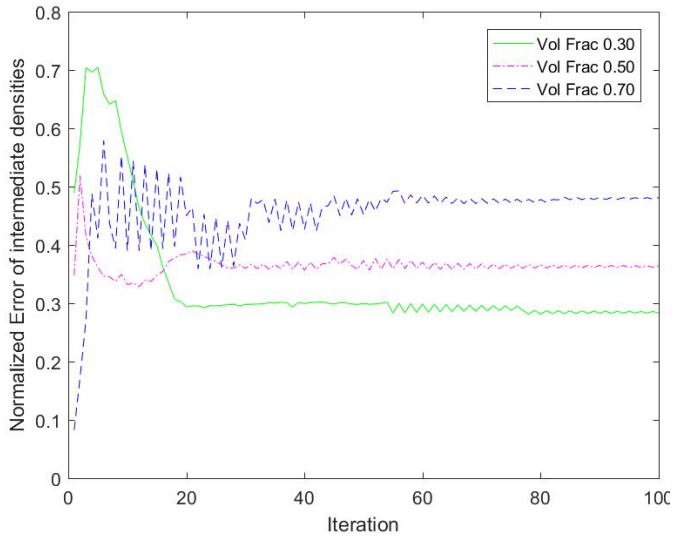

(a) Mesh of 60x20

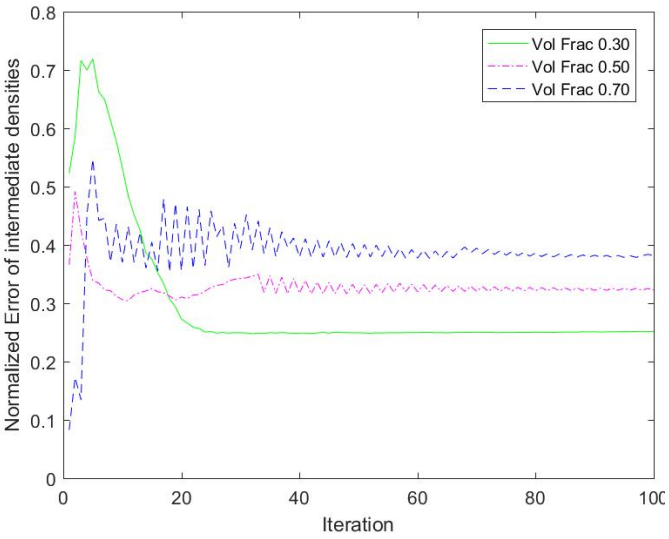

(b) Mesh of 150x50

Fig. 4.12. Normalized resolution error for MBB using Ordered SIMP.

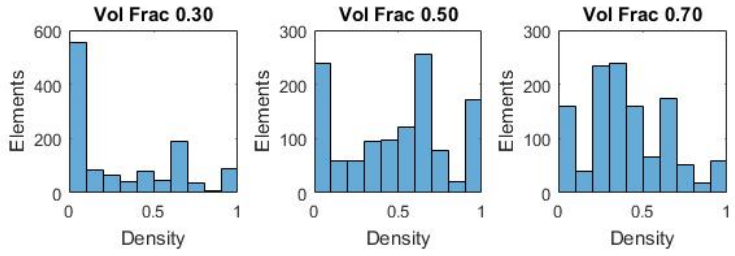

(a) Mesh of 60x20

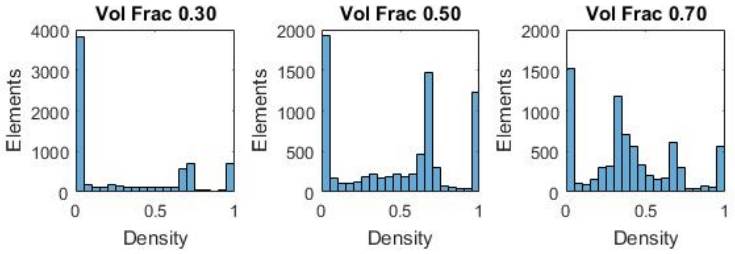

(b) Mesh of 150x50

Fig. 4.13. Density distribution for MBB using Ordered SIMP.

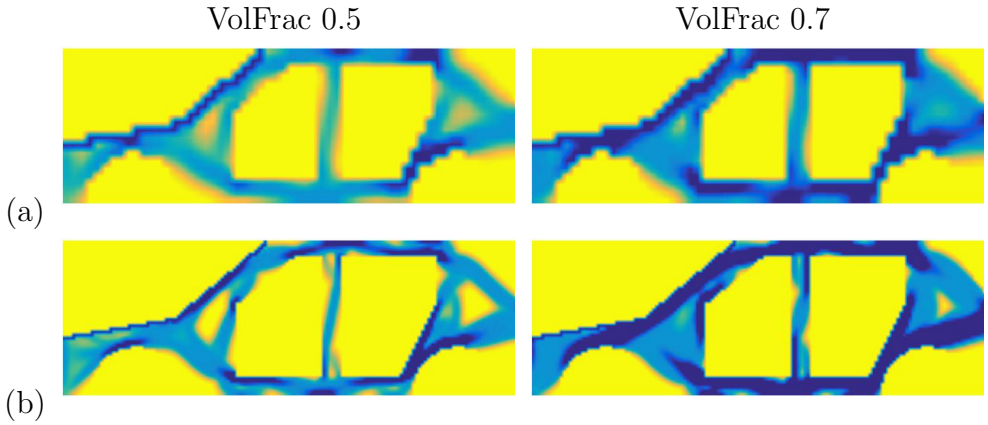

Fig. 4.14. Designs for BIW using Ordered SIMP (a)Mesh of 60x20 (b) Mesh of 150x50.

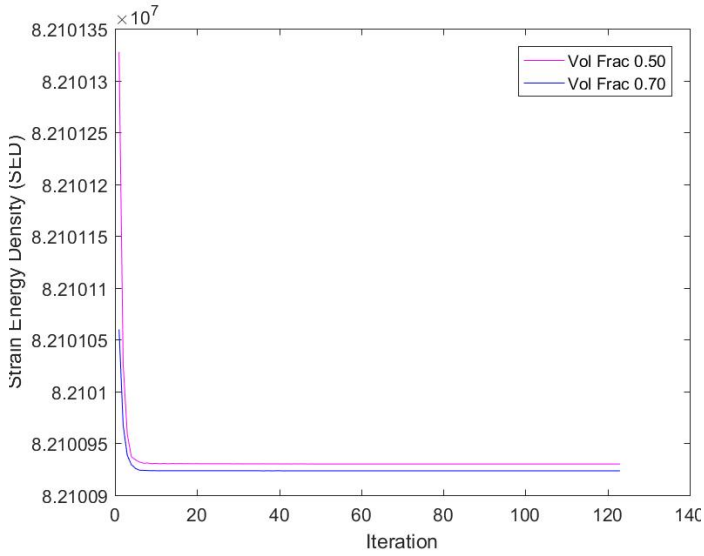

(a) Mesh of 60x20

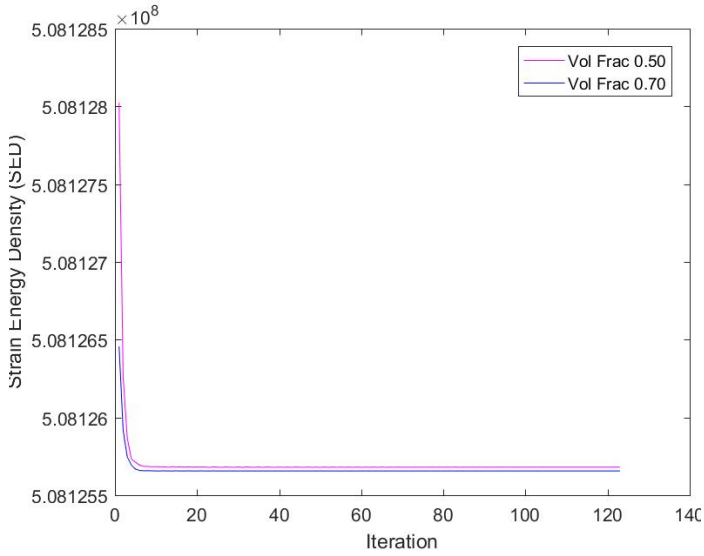

(b) Mesh of 150x50

Fig. 4.15. SED function convergence for BIW using Ordered SIMP.

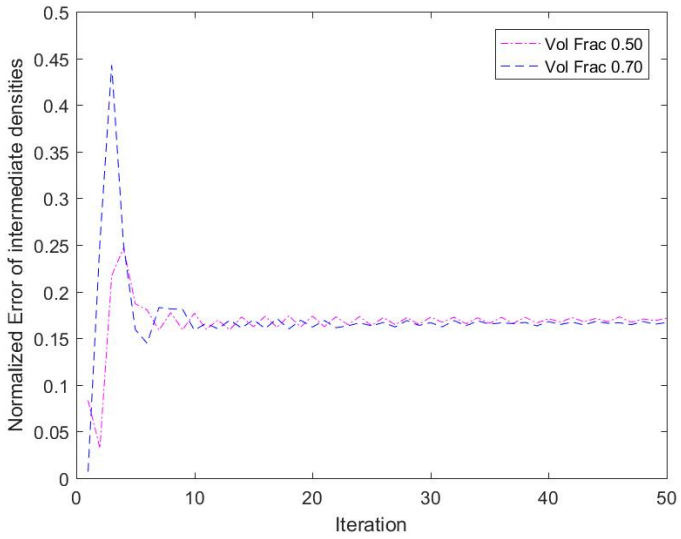

(a) Mesh of 60x20

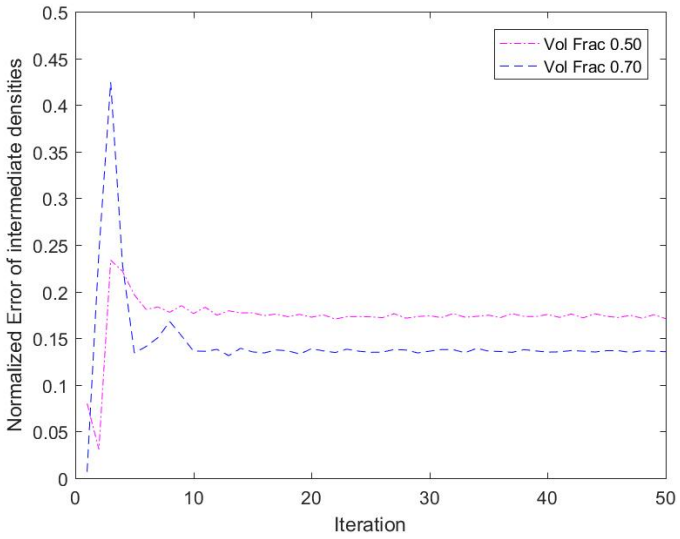

(b) Mesh of 150x50

Fig. 4.16. Normalized resolution error for BIW using Ordered SIMP.

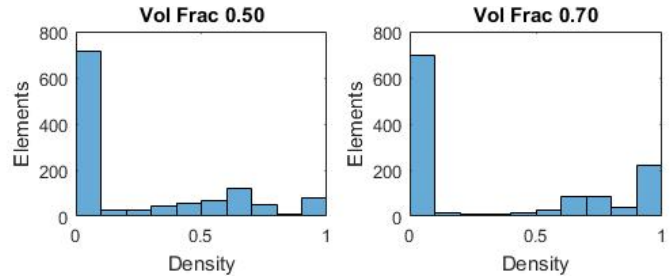

(a) Mesh of 60x20

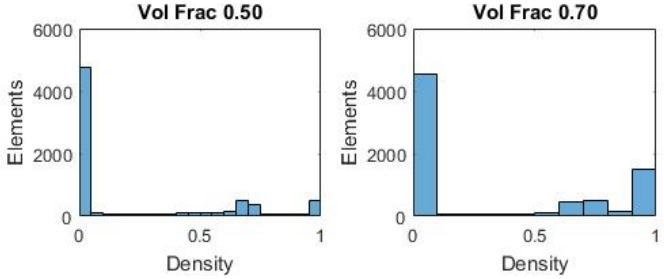

(b) Mesh of 150x50

Fig. 4.17. Density distribution for BIW using Ordered SIMP.

5. HCA FOR MULTI MATERIAL TOPOLOGY OPTIMIZATION

HCA was implemented for TO problems knowing that the solution of the Lagrangian duality for the compliance as objective function for static loading conditions, corresponds to the design where the energy per volume is constant through the mesh [20]. This algorithm present the great benefit of treating the FEA as a black box; the control system modifies the design variable with respect to the distribution of the response variable over the mesh. Since the design variable is individually updated for each finite element based on the response to that FE, there must be a correlation between the design variable and the response field. The correlation used by the authors corresponds to the well-known SIMP interpolation. SIMP has been widely used in TO as it allows relating the density of the material with its stiffness matrix. SIMP has many advantages, the main one being that since it is a continuous function, it is possible to update the design variables in a smooth manner without sudden changes, and losing information about the behavior of the design. SIMP proposes to penalize the density of the material to promote the development of binary densities, which represent void, and completely solid material. In this way, the optimization converges gradually to densities close to zeros and ones.

Nowadays, when we talk about MMTO, most of the efforts are differentiating and characterizing the phases using solely the elasticity modulus. Similarly, in this work, the phases are differentiated through the modulus of elasticity, so that the final design obtained corresponds to a solid with variable elasticity along the two dimensions. Isotropic properties and elastic behavior are assumed for the designs. Additionally, perfect bonding is assumed between the phases. The study of the bonding mechanisms and the phenomena present in the boundaries is outside the scope of this work.

5.1 Algorithm

The optimization problem for the multi-material adaptation of HCA is given by:

$$\begin{aligned} \underset{x}{\text{minimize}} \quad & S(x_i) \\ \text{subject to} \quad & \frac{\sum x_j}{nele} \leq M_f^{(m)}, \\ & \text{for } E(m) < E(x_j) \leq E(m+1) \\ & \text{with } m = 1, 2, ...M \\ & 0 \leq x_i \leq 1 \end{aligned} \tag{5.1}$$

The implementation of HCA for MMTO presented the following considerations:

• Definition of an interpolation function that allows the development of selected intermediate densities.

• Evaluation of the update rule for MMTO.

• Establishment of volume constraints for each phase, or constraints that limit the growth of the most elastic material.

5.1.1 Interpolation function

The SIMP interpolation function approximates the designs obtained to a step function, with only one step. The equivalent multi-material corresponds to a step function with as many steps as phases are considered. In view of the above Zuo and Saitou [32] proposed a step-wise formulation for a step penalized function and deduced the solution of the OC for the pice-wise interpolation rule and an additional cost constraint. On the other hand, Tavakoli and Mohseni [12] used a weighted sum of all the materials. In this case the updating of the variable can occur in a smoother manner, however, it allows the permanence of intermediate densities that do not belong to any of the considered phases.

Opting for a low computational cost, Ordered SIMP was selected as interpolation

rule. An example of interpolation function is shown in figure 5.1 for a four material optimization with normalized elasticity modulus of 0, 0.3, 0.7, and 1.

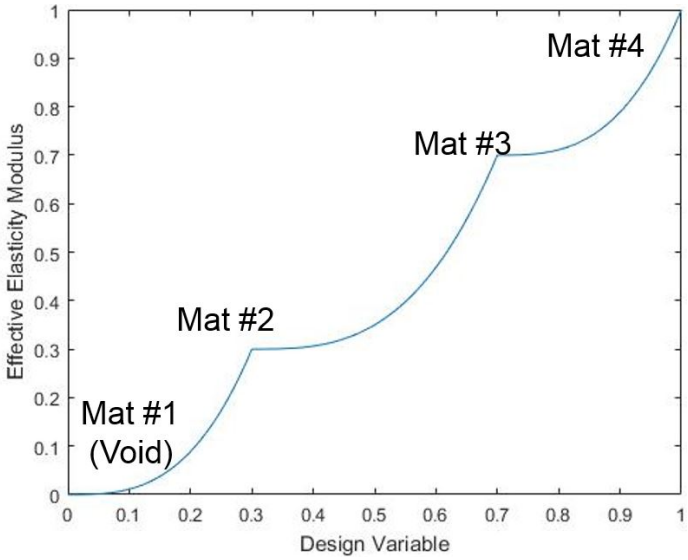

Fig. 5.1. Interpolation function for design variable and material properties.

5.1.2 Update rule

Because HCA allows the use of the FEA as a black box, the same control update rules were implemented to update the design variables. In the examples, the ratio technique and proportional rule proposed by Tovar [17] is used, as it proves to be more stable than the ordinary control rules for this specific case of small scale optimization. However, other control rules can be implemented and the tuning of the control constants must be configured according to the size of the mesh.

For the multi-material implementation, the update rule was not modified. The factor that drives the multi-material behavior of the optimization is the modification of the set point at each iteration. The set point update is explained below.

5.1.3 Volume constraint

In the traditional binary approach of TO, a volume restriction is used so that the design performance (objective function) is limited by the amount of material that can be distributed. The multi-material approach should modify this volume restriction or implement a second constraint to limit not only the quantity of material to be used, but also to favor the selection of other materials. It is evident that the stiffer material will offer the best possible performance, and the design will tend to use only this material, returning a binary solution. Tavakoli and Mohseni [12] utilized a volume fraction constraint per material, whereas Zuo and Saitou [32] introduce two additional properties to the characterization of the materials: density and cost. Leaving the cost considerations out (Cost Fraction = 1); the former work constraints the volume, and the second the mass. Both proposals are valid and have their advantages according to design considerations.

In the present work, a volume restriction per material is arbitrarily used, as in [12], so that the user indicates in a normalized vector the target volumes of each phase.This approach offers greater flexibility to the designer given that allows deciding the fractions according to various considerations and not only price. In this way, the decision of the restrictions must be a previous exercise apart from the TO problem.

HCA seeks to take advantage of the maximum use of the elements distributing the energy absorption, similar to the full stress approach. As explained previously, HCA aims to a reference SED value for all the FE called set point. If the design does not meet the volume restriction, the value of the set point increases proportionally to the ratio between the current volume fraction and the target volume fraction as presented in equation 1.9.

In the present algorithm, a set point (SP) value is sequentially defined for every material. The volume restriction is applied gradually to each material, starting with the stiffer material and ending in the less elastic material (or void). During the first iterations the set point is updated based on the volume fraction of the most elastic

material, once this restriction is fulfilled, the elements that were assigned to the most elastic material remain passive by a certain number of n_1 iterations (two, selected arbitrarily). From this point, the set point is updated using the volume fraction of the next most elastic material. After complying with the second volume fraction, likewise these elements remain passive for a certain number of iterations n_2 (three, selected arbitrarily). Following, the set point is updated based on the volume fraction constraint for the third most elastic material. This way it is performed for all remaining materials. It should be mentioned that the elements that become passive only remain in this way for a certain number of iterations to favor the convergence and direct the optimization, the elements are "released" every number of iterations to relax the problem.

Bellow is presented the pseudo-code for the multi-material implementation of HCA. The algorithm has the same structure as HCA. As mentioned above, SIMP is replaced by Ordered SIMP interpolation. The inner loop that controls the volume constraint now includes as many conditions to meet as materials are considered.

Result: final design

$S^*(t)$ calculation of Set Point

$\bar{E}(x)$ interpolated proprieties

$x(0)$ initial design

while *convergence has not been met* **do**

  $S(t)$ structural analysis FEA

  $\bar{S}(t) = f(S(t), S_N(t))$ filtered response

  while *volume constraints have not been met* **do**

    $S^*(t+1) = f(S^*(t), volfrac)$

    $e(t) = f(\bar{S}(t) - S^*(t))$

    $x(t+1) = f(x(t), e(t))$

  end

end

Algorithm 5: Multi Material HCA algorithm

5.2 Numeric examples for static loading

This section includes examples of static load simulations for the same models tested with the multi material algorithm of [12] and [34]. The boundary conditions for the MBB beam and the BIW are repeated in the Figure 5.2 below. The simulation parameters are summarized in table 5.1. To solve the optimization problems the ratio technique 1.5 was applied for the updating of the design variables since it has shown to be more stable for static loading conditions.

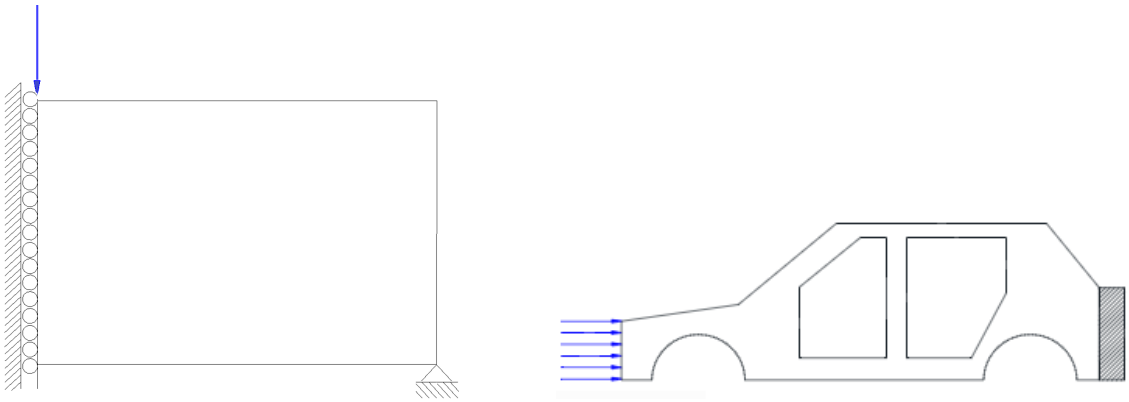

(a) MBB (b) BIW

Fig. 5.2. Simulation boundary conditions.

Table 5.1.
HCA Simulation Parameters for static simulations

Parameter	**MBB**	**BIW**
Coarse mesh	60x20	60x20
Fine mesh	150x50	150x50
Penalization	3	3
Neighbor	8	8
Elasticity Modulus	E=[1e-9 0.5 1]	E=[1e-9 0.5 1]
Vol Frac 0.30	volfrac=[0.7 0.15 0.15]	-
Vol Frac 0.50	volfrac=[0.5 0.25 0.25]	volfrac=[0.25 0.25 0.5]
Vol Frac 0.70	volfrac=[0.3 0.35 0.35]	volfrac=[0.35 0.35 0.3]

From Figures 5.3 and 5.7 can be observed that the value of the SED reaches convergence near 10 iterations. Designs for low volume fractions presented problems for convergence, displaying discontinuous structures and intermediate densities. However, for the rest of volume fractions the designs present complex solutions for the optimization problem, and successfully develop loading paths.

Figure 5.5 and Figure 5.9 shows the normalized error for undesired densities; as observed the decreased of the undesired densities takes place on a smooth manner and by the time the value of SED has converged. The nonexistence of undesired intermediate densities is expected because of the way in which the volume constraints are handled; once the volume constraint of the more elastic material is reached, those elements remain passive for a predefined number of iterations. For this study, the elements where released every 2 iterations. It was observed that the number of iterations in which the elements remain passive does not have great influence for static analysis.

The algorithm converges in a number of simulations similar to the alternating active phase. For the two sizes of mesh considered small changes in the optimization solutions are perceived.

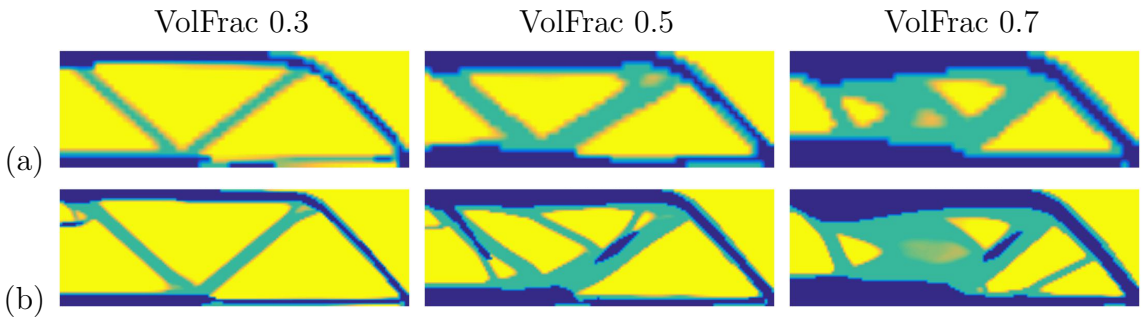

Fig. 5.3. Designs for MBB using MMTO HCA (a)Mesh of 60x20 (b) Mesh of 150x50.

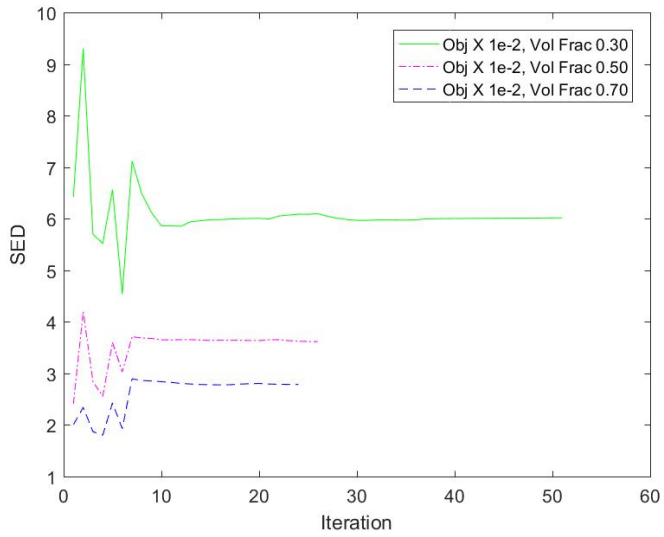

(a) Mesh of 60x20

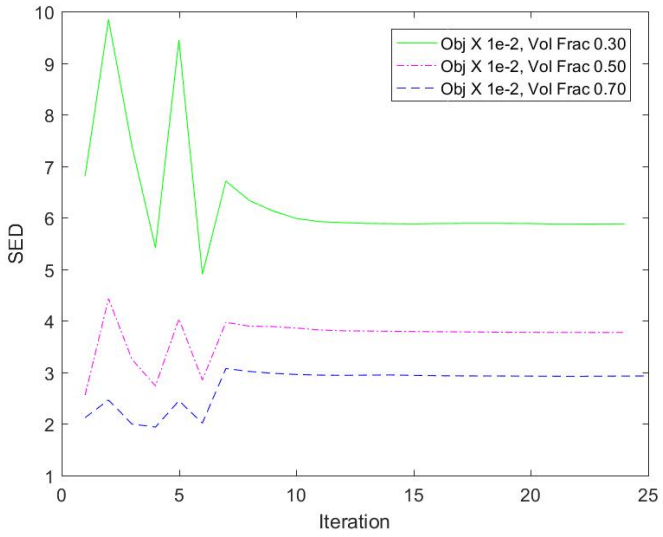

(b) Mesh of 150x50

Fig. 5.4. SED function convergence for MBB using MMTO HCA.

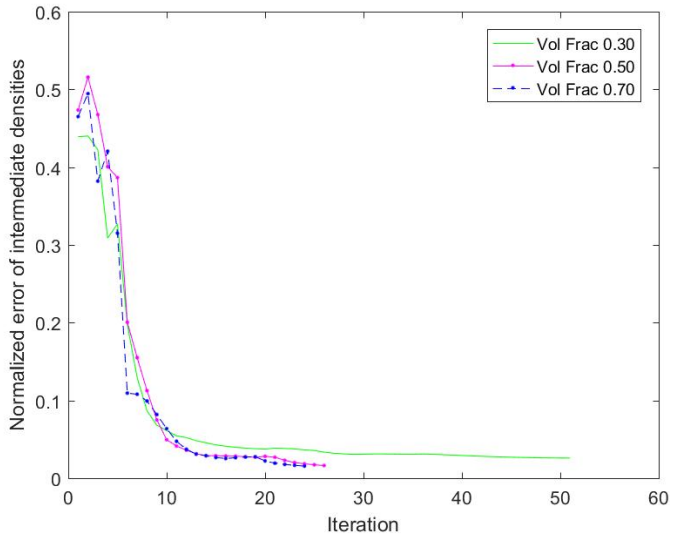

(a) Mesh of 60x20

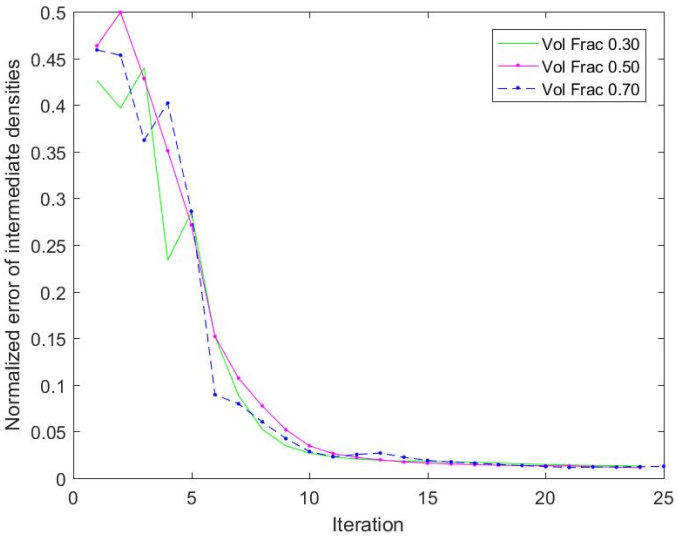

(b) Mesh of 150x50

Fig. 5.5. Normalized resolution error for MBB using MMTO HCA.

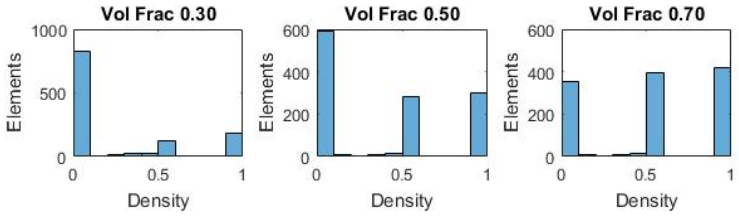

(a) Mesh of 60x20

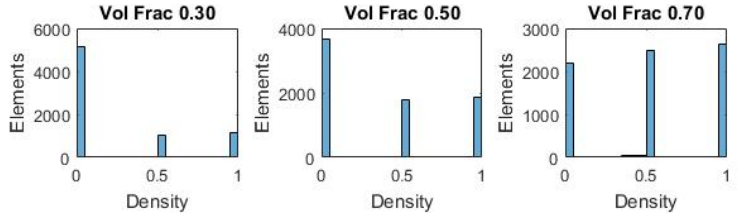

(b) Mesh of 150x50

Fig. 5.6. Density distribution for MBB using MMTO HCA.

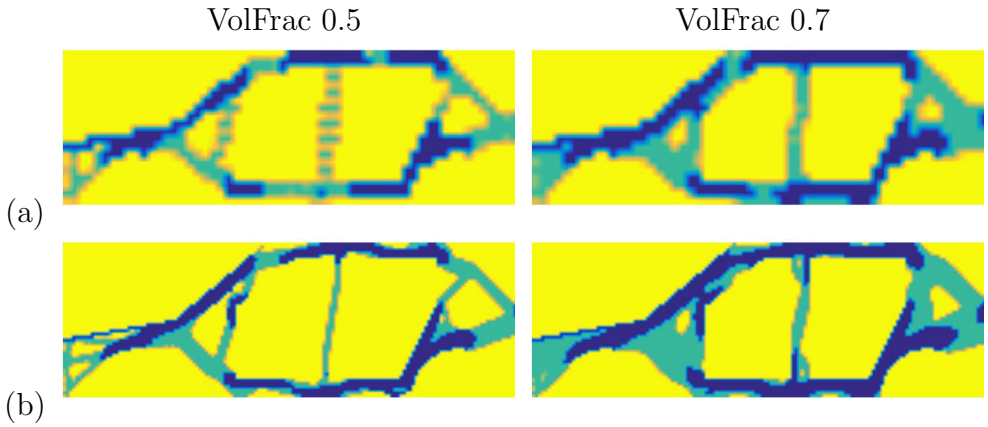

Fig. 5.7. Designs for BIW using MMTO HCA (a)Mesh of 60x20 (b) Mesh of 150x50.

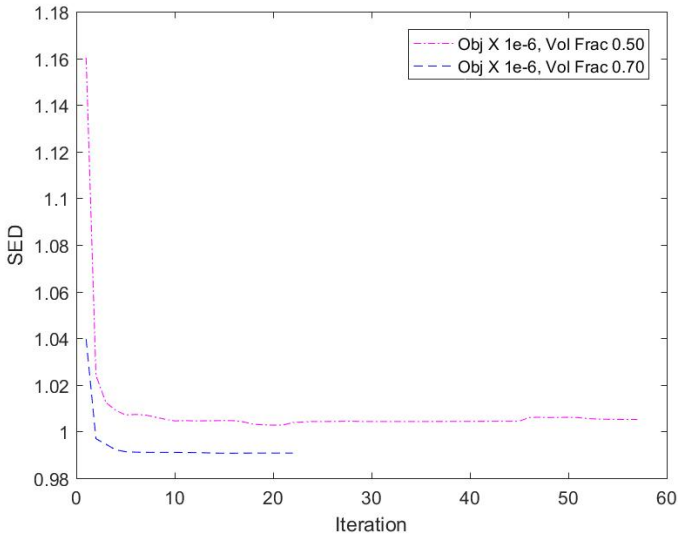

(a) Mesh of 60x20

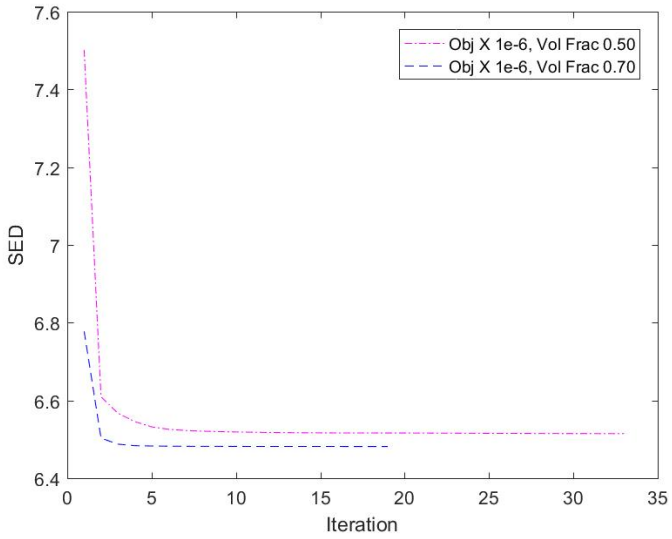

(b) Mesh of 150x50

Fig. 5.8. SED function convergence for BIW using MMTO HCA.

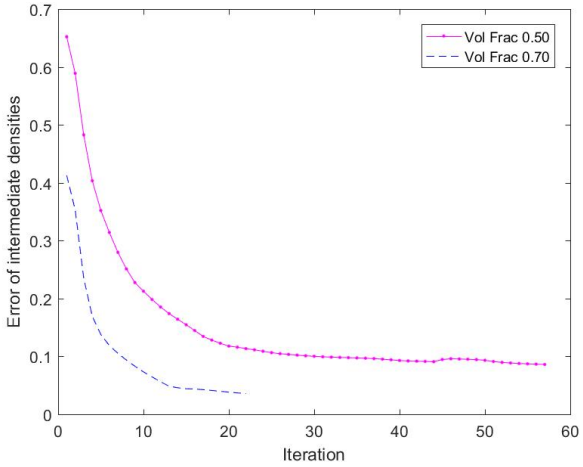

(a) Mesh of 60x20

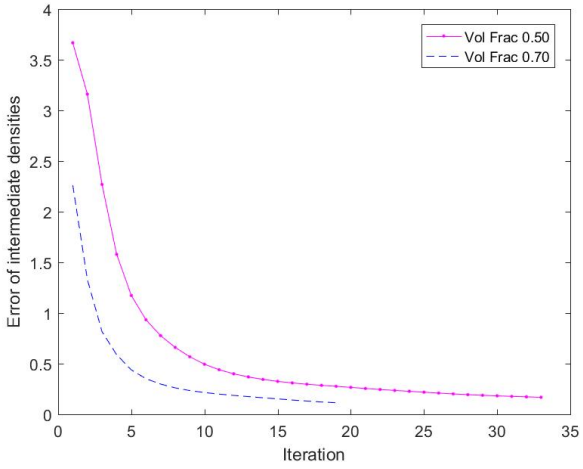

(b) Mesh of 150x50

Fig. 5.9. Normalized resolution error for BIW using MMTO HCA.

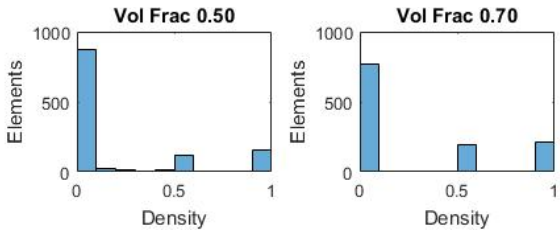

(a) Mesh of 60x20

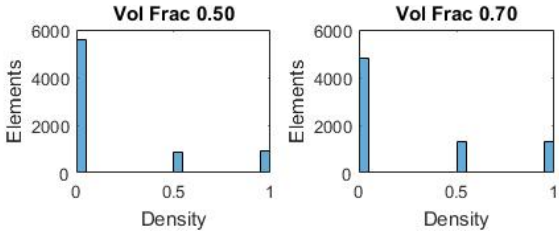

(b) Mesh of 150x50

Fig. 5.10. Density distribution for BIW using MMTO HCA.

6. HCA FOR MULTI MATERIAL CRASHWORTHINESS TOPOLOGY OPTIMIZATION

This section presents the multi-material adaptation of HCA for impact loads. The first part explains the modifications made to the multi-material HCA to optimize dynamic loads, these modifications are based on Patel's proposal [37]. The second part covers the considerations taken in the models to perform the dynamic simulations using the commercial software Ls-Dyna. Following, two examples of multi-material topology optimization for quasi- static loads are given, and the chapter closes with optimization examples for impact loads.

6.1 Algorithm

The HCA multi-material algorithm previously demonstrated for static loads, was modified based on Patel's proposal [37] to optimize designs under dynamic load. Below is presented the pseudo-code for multi-material HCA for crash-worthiness.

Result: final design

$S^*(t)$ calculation of Set Point

$\bar{E}(x)$ interpolated proprieties

$x(0)$ initial design

while *convergence has not been met* **do**

  $S(t)$ structural analysis FEA

  $\bar{S}(t) = f(S(t), S_N(t))$ filtered response

  $\bar{S}_h(t) = f(\bar{S}(t), \bar{S}(t-1), \bar{S}(t-2), \bar{S}(t-3))$ response memory

  while *volume constrainst have not been met* **do**

    $S^*(t+1) = f(S^*(t), volfrac)$

    $e(t) = f(\bar{S}_h(t) - S^*(t))$

    $x(t+1) = f(x(t), e(t))$

  end

end

Algorithm 6: Multi material HCA algorithm for crashwrothiness

The algorithm maintains the same structure as HCA. The main change is the response managing. As performed in the original HCA, once the response is obtained from the FEA black box, it is filtered with respect to the neighborhood responses. For dynamic loads, Patel recommends using the response history to perform the update of the design variable. The response of each element is given by a weighted sum of the response of the element in the present iteration and three previous iterations. This weighted sum is expressed in equation 3.4. The history of the response allows to reduce the oscillations in the optimization process and benefits the convergence. Since the response is expressed as a weighted sum with respect to the densities of the element, the elements with low densities (close to zero), will have little memory of previous states; this allows the regeneration of the voids if required by the mesh in future iterations.

The design variables are related to the material properties by the interpolation function based on meta-model proposed for the multi-material optimization. As for the variable update rule, the algorithm can potentially work with any of the control rules previously shown in the equation 1.5. However, in this work, only the proportional rule was used for dynamic loading. The proportional rule was recommended in Patel's work [37] and was also implemented in the commercial software LS-Tasc [45]. In this way, the proportionality variable must be tuned according to the conditions of the simulation problem.

Based on the experience gained from the use of the algorithm, it was concluded that the user must properly tune three variables:

• The recently mentioned proportionally constant for the update rule. This dictates the magnitude of the change in design variables. It is advisable to make changes gradually to the structure so that the response field likewise does not vary much. The update of the design variable depends on the history of iterations if the response variable is very different between iterations, the update lacks trend.

• The time of design which corresponds to the time in which the response is compile. For dynamic problem, the response is transient and different for each time. Later in this section, dynamic simulations are shown with three different design times. For future collaborations, we propose to analyze the performance of the algorithm using history of iterations but also including the history of design times, so that the solution considers the behavior at different times. Possibly, this greatly increases the complexity and destabilizes the solution of the optimization problem.

• Number of iterations to release the volume fraction restriction. This variable relaxes or stiffens the design solutions since it minimizes a number of elements that can be updated.

6.2 Ls Dyna Integration

The commercial software Ls-Dyna was used as a black box to obtain the response of the models. LS Tasc is a topology and shape optimizer that works with the Ls-Dyna solvers, it implemented HCA algorithm to optimize designs under crash events [45]. The integration of Ls Dyna into the MMTO HCA algoritm used the Ls Tasc scheme to handle the simulation files.

The implementation of HCA for crash events works for two dimensional designs, solid elements and under elastic behavior. The optimization is performed using Matlab in two dimensions, then Ls-Dyna is used as a black box for testing the designs and obtaining the field response. To simulate the crash in Ls-Dyna, the designs must be converted into three dimensional models, so the two dimensional designs are extruded using little elements enough to avoid buckling. However, the code can be expanded for tri-dimensional designs by modifying the HCA functions such as the filter. The major challenge is to carefully perform the mapping of the design variables into the Ls-Dyna mesh.

The optimization code modifies the input files of Ls-Dyna, called k file (key file), in each iteration. This file contains the model of the simulation, as the details of the mesh, loads, boundary constraints, contacts, simulation time, desired output information, etc. The code modifies the modulus of elasticity of each element, and after the simulation it collects the value of the SED of each element from the d3plot output file.

As known, the density approach optimization allows the existence of intermediate densities to relax the problem. In order to be consistent with the continuous optimization update, the Ls-Dyna input file is created with 100 material cards. The material card number 1 represents a material with an elasticity modulus near zero (void), whereas the material card 100 corresponds to the stiffer material. For this model, the the properties of steel were assumed for the material with the card number 100. In the same way, the input file uses as many part cards as number of material

cards. In each simulation, the parts assigned to each element of the mesh are modified, which therefore modifies the mechanical properties of the element.

The elements that are assigned with the void material are removed from the mesh to avoid numerical instabilities due to large deformations, as recommended by [45]. The elements have the possibility to re-grow in future iterations if necessary, while they are eliminated they are assigned a response of zero.

Another important consideration for impact simulations are contacts. The model includes two different types of contacts. The first one corresponds to the contact between the design and the rigid wall (or pole) that impacts it. The second type of contact occurs between the same elements of the design when the material is deformed. This contact must be defined only between the active parts of the design to avoid errors in the simulation. In this way, after each iteration in addition to modifying the parts of each element of the mesh, the code must update the set of active parts to feed the contact card.

6.3 Numeric examples for dynamic loading

This section includes dynamic loading examples for the MMTO HCA algorithm. Ls-Dyna was used as solver for the FEA. The impact was set using a pole as rigid wall and imposing a prescribed displacement. The boundary conditions are shown in the Figure 6.1. The first model corresponds to a cantilever beam impacted at the end; the second model corresponds to a bumper impacted at the middle of its length, the problem was solved by symmetry modeling only half of the bumper. The simulation parameters are summarized on table 6.1 and table 6.2. The Figure 6.2 shows the curve that defines the prescribed displacement for the pole that works as a rigid wall; the axis of the abscissa corresponds to the time of simulation and the axis of the ordinates to the displacement in meters. All units used for the Ls Dyna simulation correspond to the International System of Units and are given in: kg-m-s-N-Pa-J.

Table 6.1.
HCA Simulation Parameters for impact simulations

Parameter	**Cantilever**	**Half Bumper**
Mesh size	150x50	150x50
Penalization	3	3
Neighbor	8	8
Proportional Gain	0.05	0.05
Elasticity Modulus	E=[1e-9 0.5 1]	E=[1e-9 0.5 1]
Vol Frac 0.30	volfrac=[0.7 0.15 0.15]	volfrac=[0.7 0.15 0.15]
Vol Frac 0.50	volfrac=[0.5 0.25 0.25]	volfrac=[0.25 0.25 0.5]
Vol Frac 0.70	volfrac=[0.3 0.35 0.35]	volfrac=[0.35 0.35 0.3]

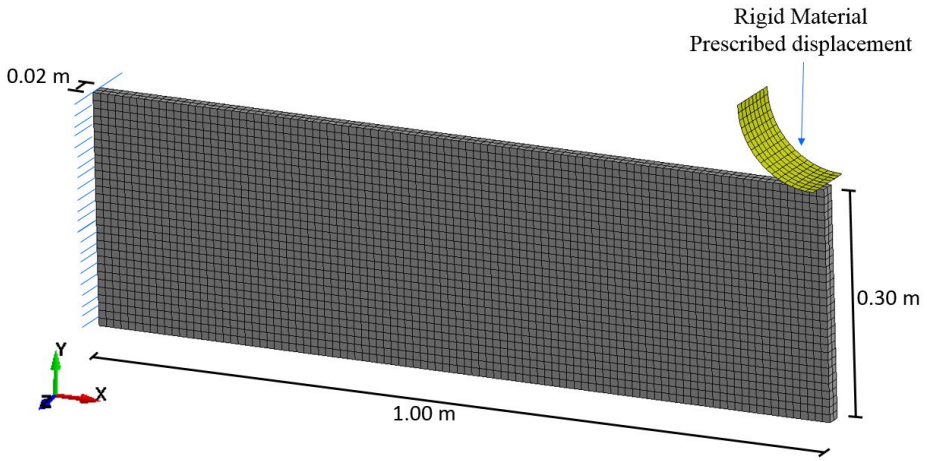

(a) Cantiliver

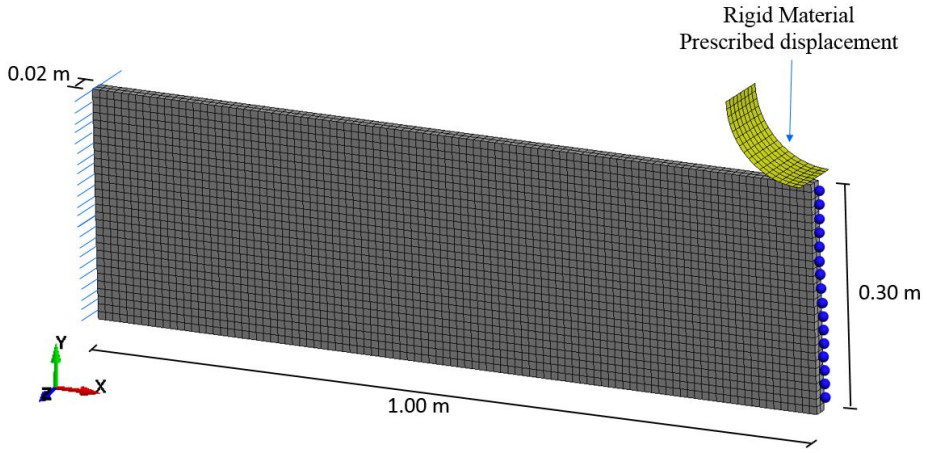

(b) Half Bumper

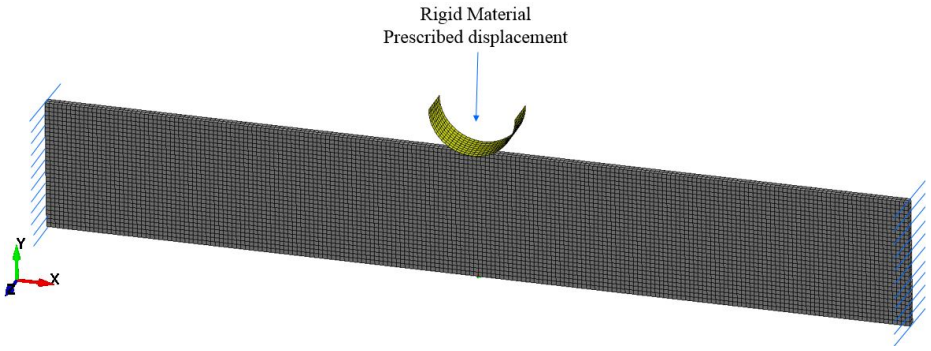

(c) Bumper

Fig. 6.1. Dynamic simulation boundary conditions.

Table 6.2.
Ls Dyna Simulation Parameters for impact simulations

Termination time	1e-2 s
Load	Nodal load
Elasticity Modulus	2.07e+11 Pa
Density	7830 kg/m^3
Poisson ratio	0.3

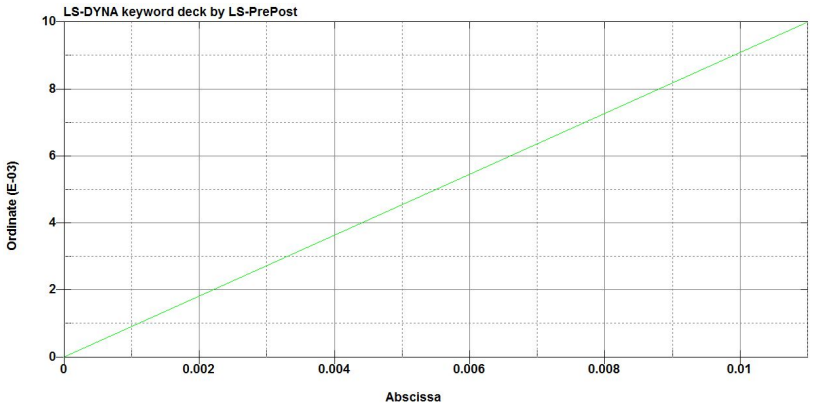

Fig. 6.2. Prescribed displacement for pole (rigid wall).

6.3.1 Beam under transverse impact

The Figure 6.3 shows the designs obtained for the cantilever beam impacted by the pole. Only the solutions for three volume fractions are presented since the model with volume fraction 0.1 did not converge, it was composed by discontinuous structures. This bad performance was previously observed for low volume fraction designs for the simulations under static loads. It seems that the complexity of the dynamic load response field does not allow a continuous structure to be generated even if it would include intermediate densities.

For the volume fractions present, complex structures are again observed. The designs are characterized by distributing the most elastic material on the surface where there

is greater stress of compression and tension. The resolution error decreases smoothly as seen in Figure 6.4, and converges by the time the SED converges. As in the static case, there are few or no undesired intermediate densities (Figure 6.5. The convergence is more unstable than in static cases, and although the optimization requires more iterations to converge, the solution is found in about 50 iterations (Figure 6.6. As mentioned previously, the HCA code has two loops. The outer loop controls the iterations and convergence of the objective function, while the inner loop controls the volume constraints. Figure 6.6b shows the history of internal loops required to comply with the volume constraint. The optimization iterates less than 100 times before finding a suitable update of the design variables. Finally, Figure 6.7 shows the elemental SED distribution along the design for the two different solid materials. As observed, the internal energy of is equalized for the materials that are assigned with one same material.

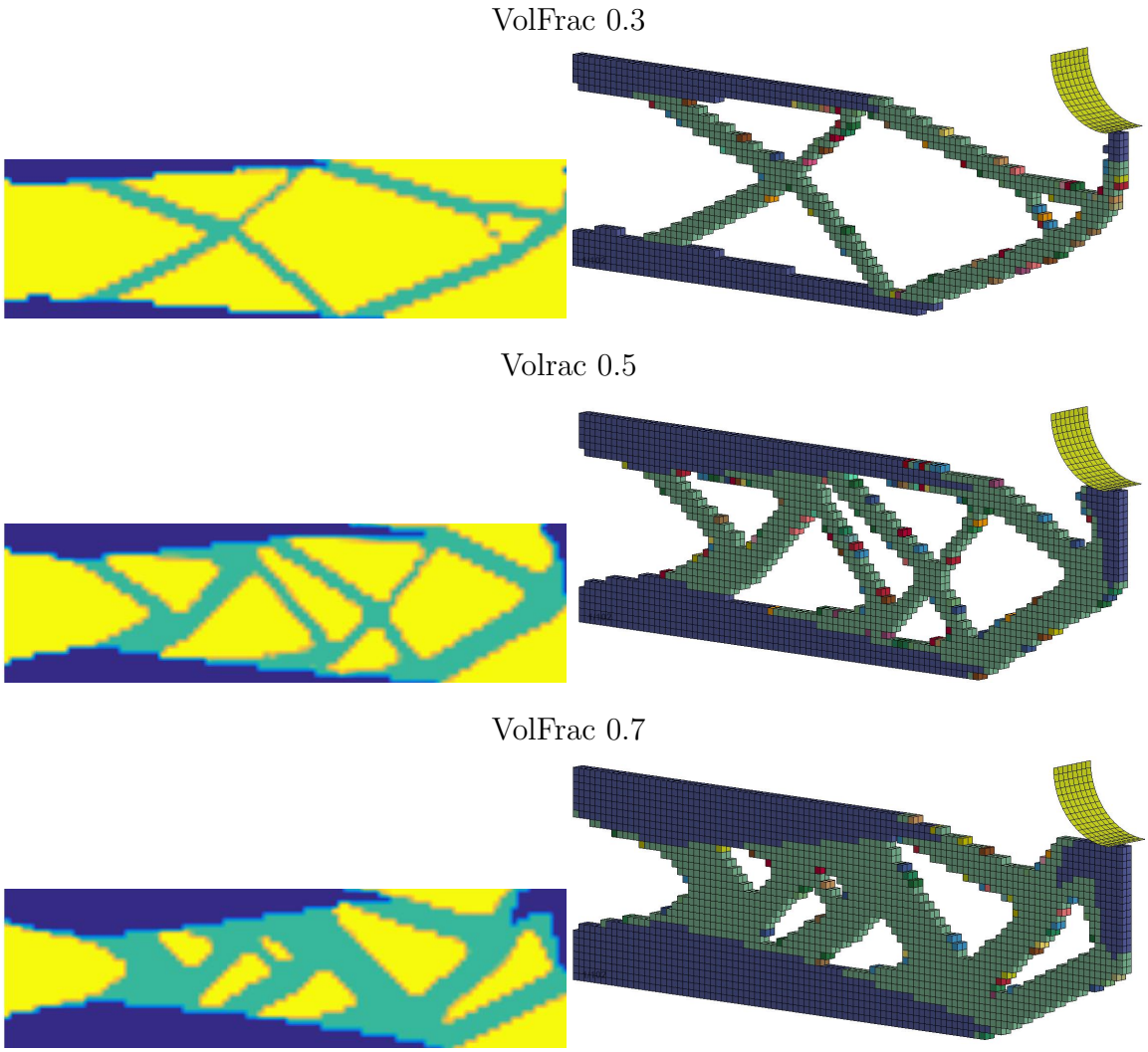

Fig. 6.3. Cantilever beam under impact load using MMTO HCA. The design on the left side corresponds to the 2D Matlab model and design on the right to the 3D Ls Dyna model.

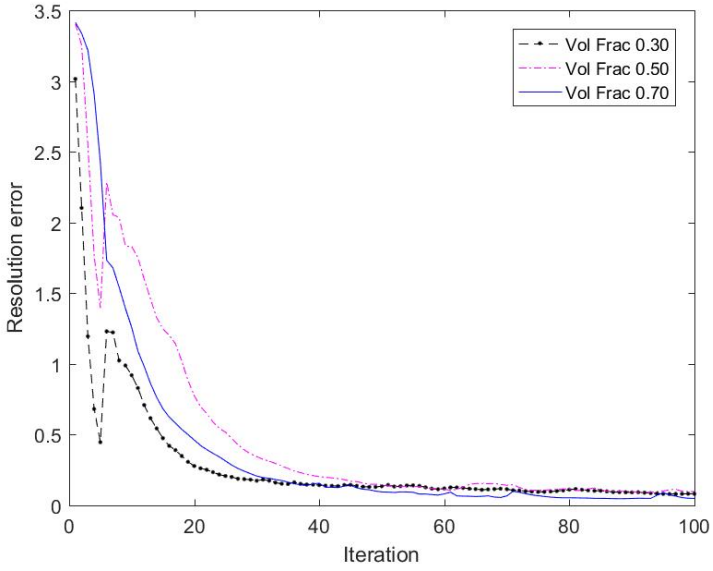

Fig. 6.4. Normalized resolution error for cantiliver beam using MMTO HCA.

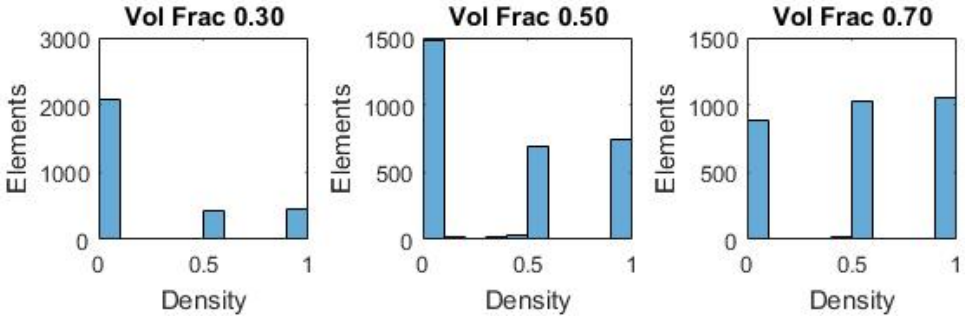

Fig. 6.5. Density distribution for cantilever beam under transverse impact using MMTO HCA..

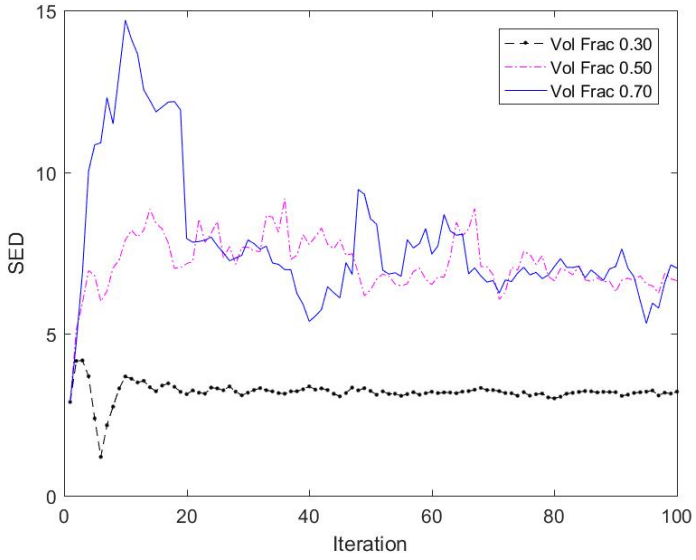

(a) Mesh of 60x20

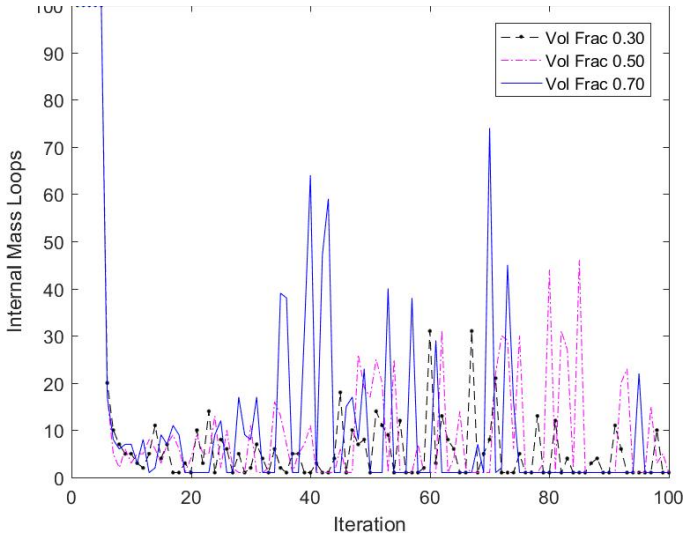

(b) Mesh of 150x50

Fig. 6.6. Convergence for cantilever beam under transverse impact using MMTO HCA.

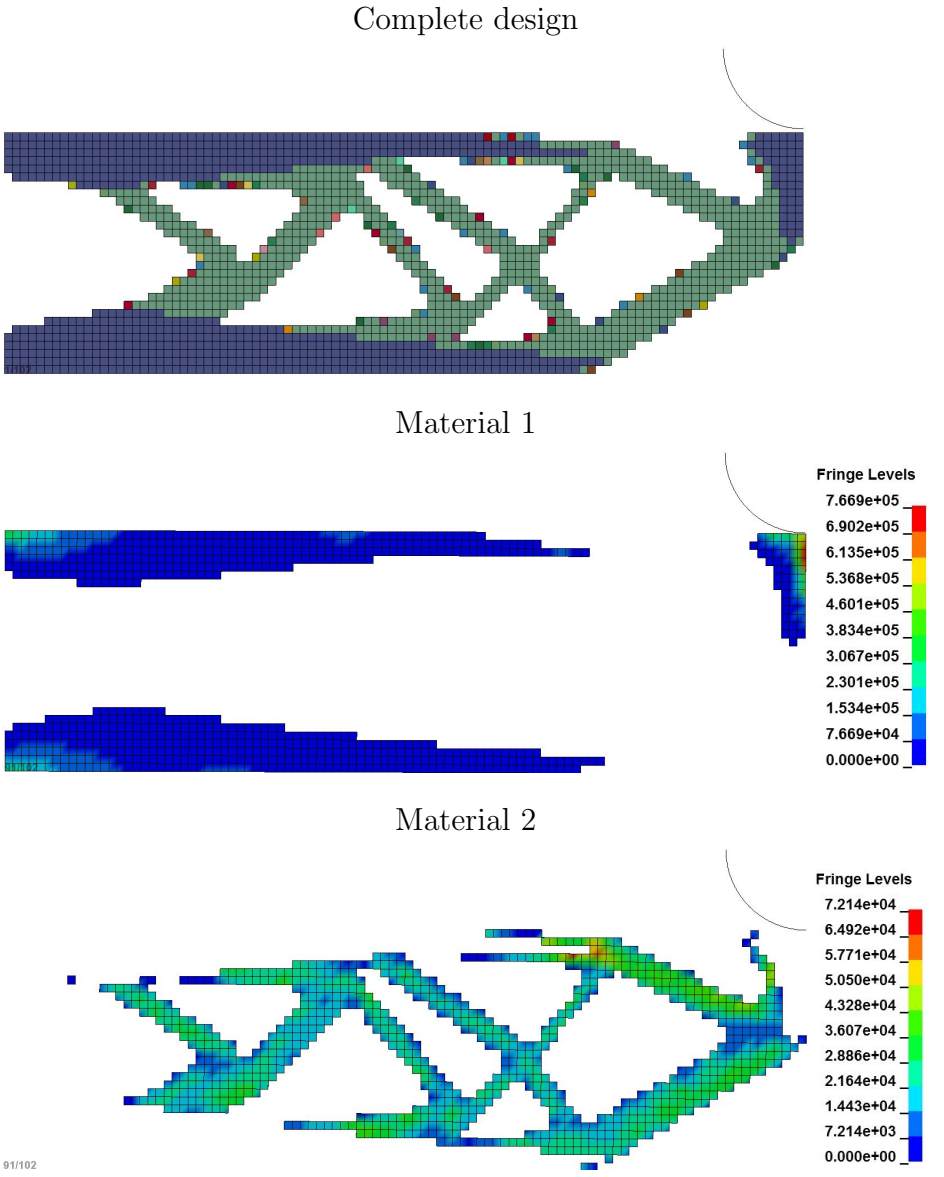

Fig. 6.7. SED distribution for the cantilever beam under impact load using MMTO HCA.

6.3.2 Bumper under transverse impact

The bumper simulation was performed using symmetry conditions. The third column of Figure 6.8 shows the complete design of the bumper with the pole impacting it in the middle. The first two columns show the model used to perform the optimization. Of the three simulations, the design with a volume fraction of 0.3 shows a defect with a discontinuous section that does not offer any mechanical advantage.

Figure 6.9 shows that the resolution error behaves similarly to the previous cases studied. Undesired intermediate densities are almost non existent (Figure 6.10; the solution continues to offer a density distribution more favorable to that observed with other algorithms of multi-material optimization.

In this case, the maximum number of design iteration was set to 200, however the value of the SED continuous oscillating after 100 iterations. The results shown in the Figure 6.11 correspond to the most representative behavior of the optimization. This optimization problem is more complex than that of the cantilever beam; despite of this fact the loops required to meet volume constraints continue to be less than 100 iterations. The number of mass iterations, corresponding the inner loop, are less than the maximum number of internal loop iteration admissible of 100 .

The Figure 6.12 shows the distribution of the elemental SED for one same solid material. As in the example for the cantilever beam, MMTO HCA minimizes the dispersion of the response for the considered elements in the mesh.

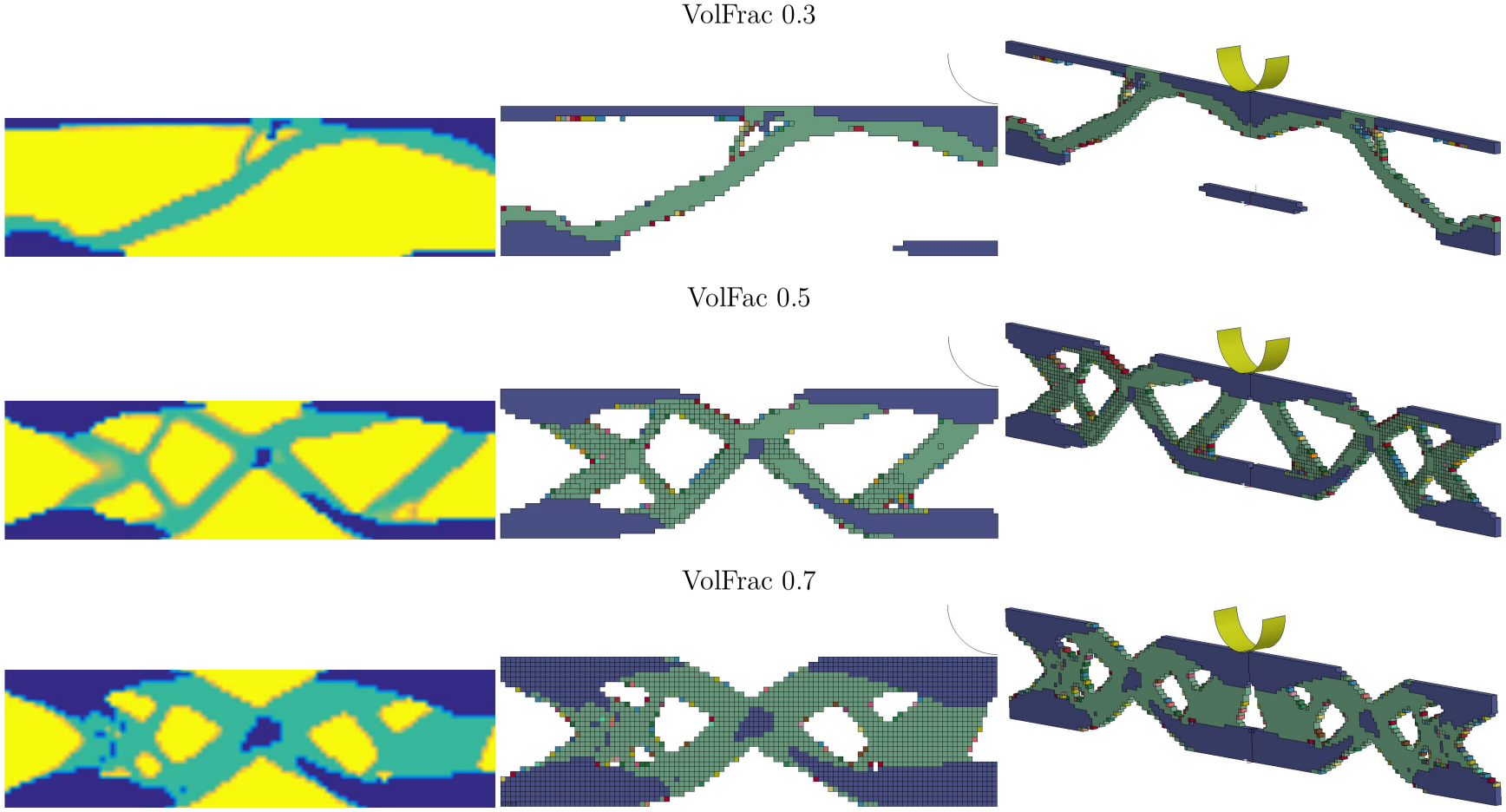

Fig. 6.8. Bumper under impact load. The design on the left side corresponds to the 2D Matlab model and the two designs on the right to the 3D Ls Dyna model.

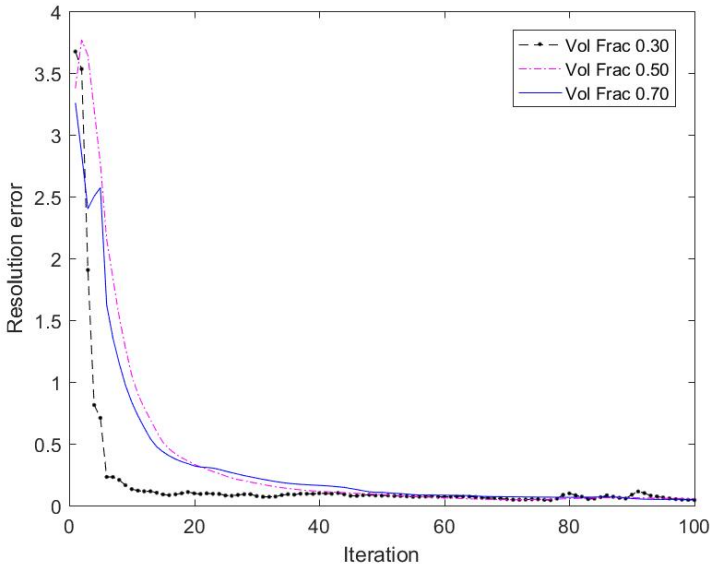

Fig. 6.9. Normalized resolution error for half bumper using MMTO HCA.

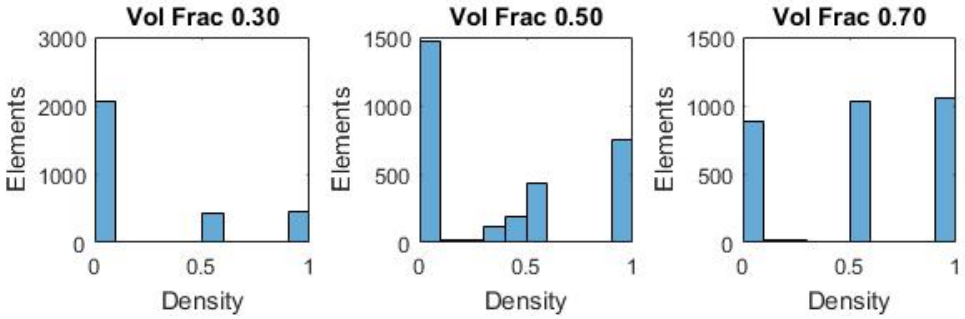

Fig. 6.10. Density distribution for half bumper under transverse impact using MMTO HCA..

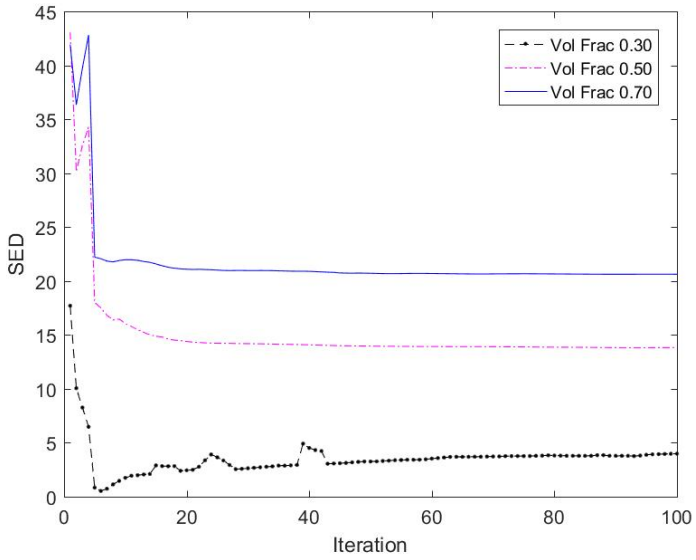

(a) Mesh of 60x20

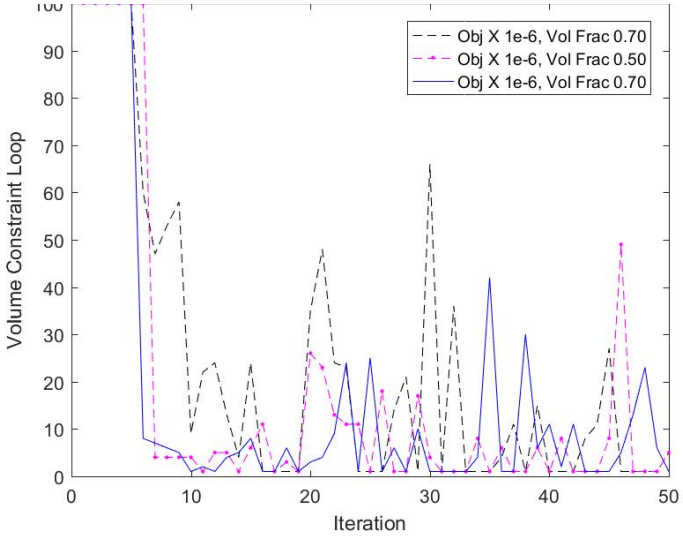

(b) Mesh of 150x50

Fig. 6.11. Convergence for half bumper under transverse impact using MMTO HCA.

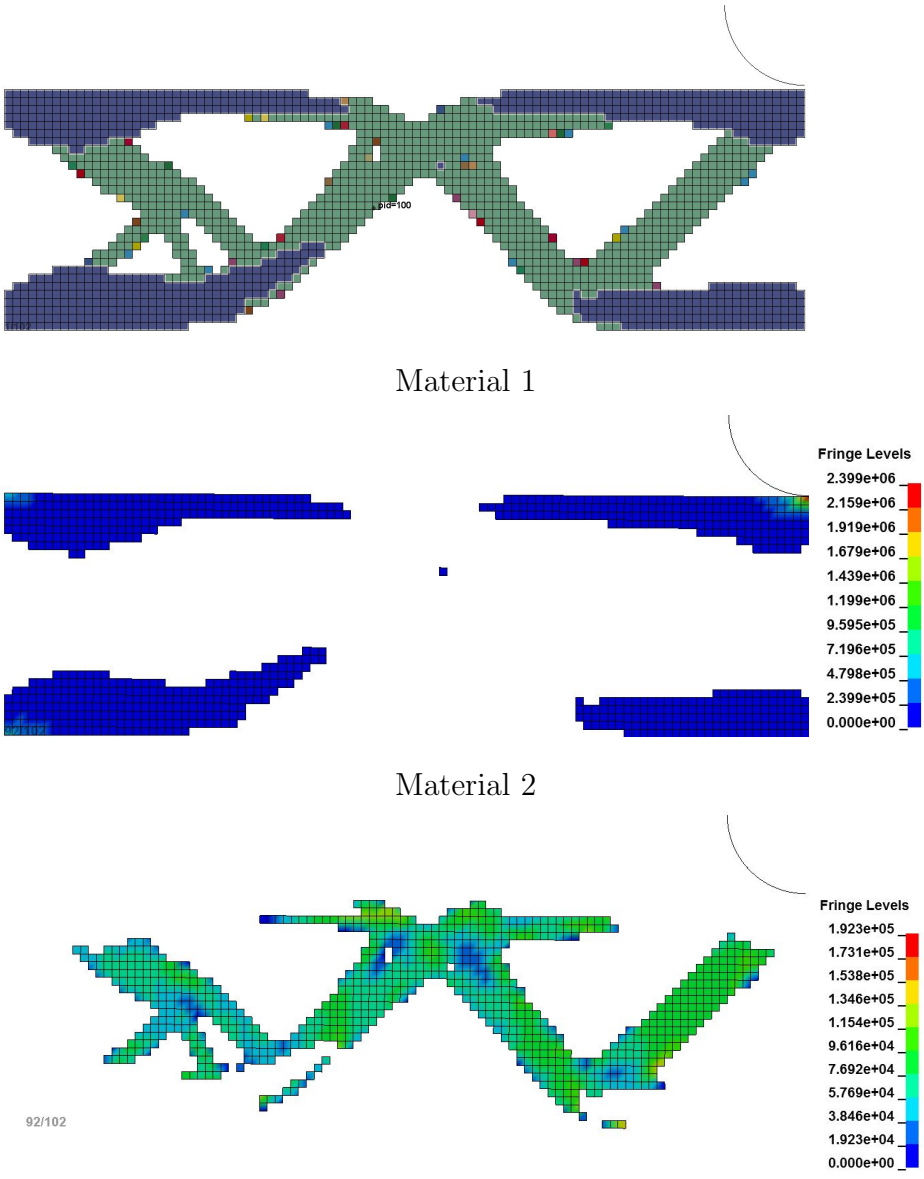

Fig. 6.12. SED distribution for half bumper under impact load using MMTO HCA.

6.3.3 Design time influence in the design solution

The model of the cantilever beam was run three different design times, considering the rest of parameters fixed. The beam model uses a volume fraction of 0.5. The objective of this numeric example is to show the influence that both parameters have on the optimization solutions.

The results obtained are shown in the Figure 6.13. At different times the response field at different times varies so the optimization solutions are different. Although the convergence graph indicates that the objective function converges faster and lower response values are obtained, it is difficult to obtain conclusions about the time required to perform the optimization. During the analysis process, other simulation times were taken to which the design did not converge. For this reason, it is important to make an analysis of the design time that best suits according to the application of the design. For future collaborations it is possible to analyze the performance of the algorithm when considering the history of states (times), so that the design has to comply with the response to different times. As mentioned previously, this additional consideration could significantly increase and impair the convergence of the code to a solution. However, the possibility may be considered due the little information and the uncertainty that exists regarding the optimum design time.

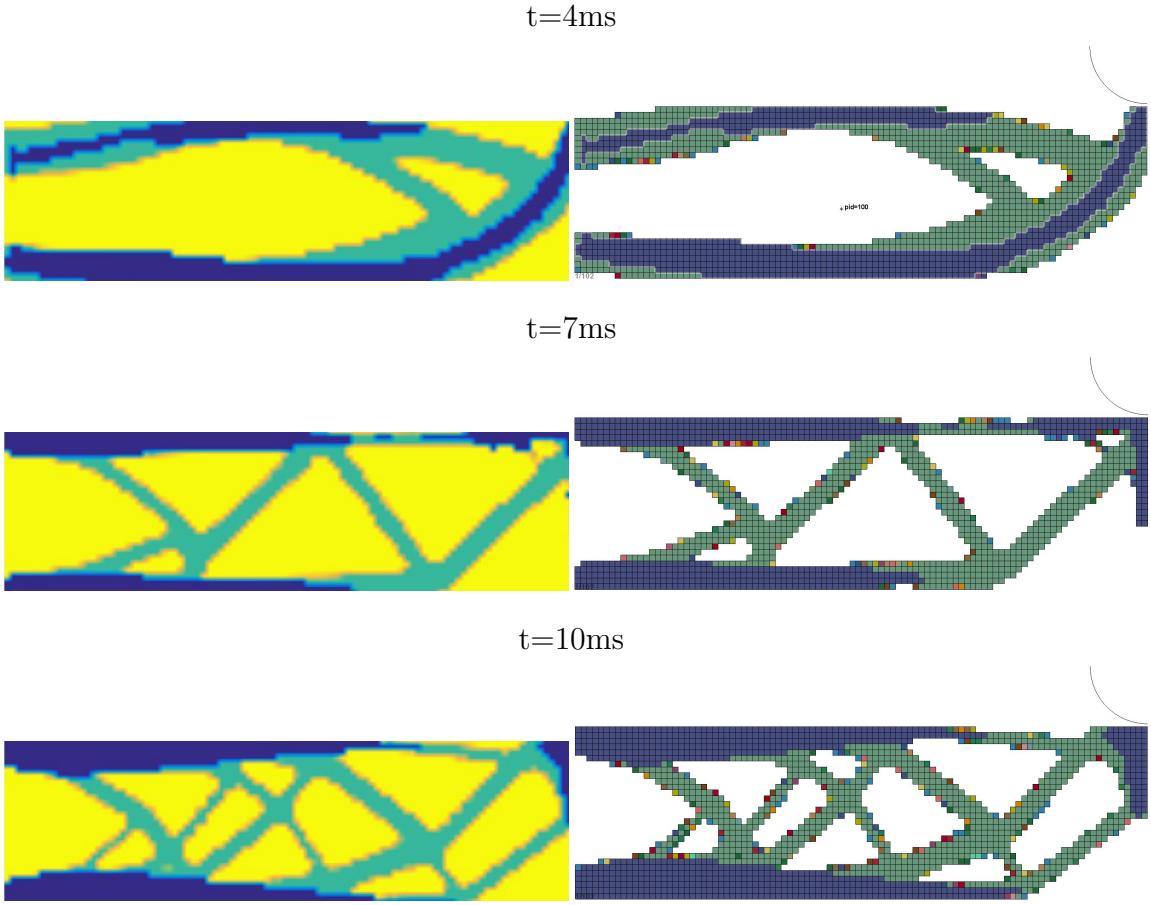

Fig. 6.13. Cantilever beam under impact load for different design times. The design on the left side corresponds to the 2D Matlab model, and design on the right to the 3D Ls Dyna model.

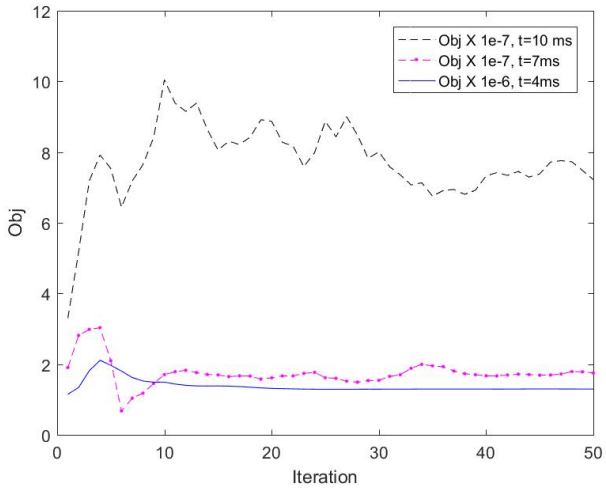

Fig. 6.14. Objective function convergence for different impact velocities

7. SUMMARY AND RECOMMENDATIONS

Topology optimization allows to develop designs with complex topologies that maximize the use of the materials. In addition to optimizing the binary distribution of solid material and void, it is possible to appeal for the distribution of several phases that together offer mechanical, cost or weight advantages. The multi-material topology has been developed in previous works expanding the different approaches of density based, set level, and phase field.

HCA is a density-based algorithm for topology optimization with a control-system-based solver, inspired in the bone regeneration process. HCA has been used to successfully solve optimization problems under static load and impact loads. The present work expanded the use of HCA for multi material topology optimization applications. The algorithm replaces the SIMP interpolation with ordered SIMP interpolation function, which allows to relate the design variables to the mechanical properties of the material. To perform the actualization of the variables during each iteration, the ratio rule was used for static loads, and the proportional rule was tested for dynamic loading conditions. The user decides the volume fraction for each material. Volume constraints are applied sequentially starting with the most elastic material. Cells that belong to the material that has already met the volume restriction remain passive for a certain number of iterations to promote the convergence of the solution. Numerical examples are included for cases of static and dynamic load. For the cases of impact loading it is observed that the designs obtained depend to a large extent on the design time and the impact speed.

The proposed algorithm has a series of parameters that must be tuned, particularly for the transient loading conditions. The first corresponds to the control system gains according to the rule that is applied. The second parameter corresponds to the number of iterations in which the elements remain passive during the volume constraints.

The third parameter corresponds to the design time, which also for transient loads. Several of these parameters depend on the application and the preference of the designer; however, the influence can be more explored.

Finally, the optimization assumes perfect bonding between the phases. Future works may focus on analyzing the shear stresses that are involved in joints, and assign a maximum value as a constraint on optimization.

REFERENCES

REFERENCES

[1] M. P. Bendsøe and N. Kikuchi, "Generating optimal topologies in structural design using a homogenization method," *Computer Methods in Applied Mechanics and Engineering*, vol. 71, no. 2, pp. 197–224, 1988.

[2] M. Zhou and G. Rozvany, "The coc algorithm, part ii: Topological, geometrical and generalized shape optimization," *Computer Methods in Applied Mechanics and Engineering*, vol. 89, no. 1-3, pp. 309–336, 1991.

[3] H. Mlejnek, "Some aspects of the genesis of structures," *Structural and Multidisciplinary Optimization*, vol. 5, no. 1, pp. 64–69, 1992.

[4] A. Aremu, I. Ashcroft, R. Hague, R. Wildman, and C. Tuck, "Suitability of simp and beso topology optimization algorithms for additive manufacture," in *Twenty First Annual International Solid Freeform Fabrication Symposium, Austin*, 2010, pp. 679–692.

[5] H. Long, Y. Hu, X. Jin, H. Yu, and H. Zhu, "An optimization procedure for spot-welded structures based on simp method," *Computational Materials Science*, vol. 117, pp. 602–607, 2016.

[6] L. Grekavicius, J. A. Hughes, K. D. Tsavdaridis, and E. Efthymiou, "Novel morphologies of aluminium cross-sections through structural topology optimization techniques," in *Aluminium Constructions: Sustainability, Durability and Structural Advantages*, no. 710. Trans Tech Publications, 2016, pp. 321–326.

[7] S. Yu, C. Wang, C. Sun, and W. Chen, "Topology optimization for light-trapping structure in solar cells," *Structural and Multidisciplinary Optimization*, vol. 50, no. 3, pp. 367–382, 2014.

[8] S. Osher and J. A. Sethian, "Fronts propagating with curvature-dependent speed: algorithms based on hamilton-jacobi formulations," *Journal of Computational Physics*, vol. 79, no. 1, pp. 12–49, 1988.

[9] J. A. Sethian, *Level set methods and fast marching methods: evolving interfaces in computational geometry, fluid mechanics, computer vision, and materials science*. Cambridge University Press, 1999, vol. 3, pp.1-2.

[10] M. Y. Wang, X. Wang, and D. Guo, "A level set method for structural topology optimization," *Computer Methods in Applied Mechanics and Engineering*, vol. 192, no. 1, pp. 227–246, 2003.

[11] G. Allaire, F. Jouve, and A.-M. Toader, "A level-set method for shape optimization," *Comptes Rendus Mathematique*, vol. 334, no. 12, pp. 1125–1130, 2002.

[12] R. Tavakoli and S. M. Mohseni, "Alternating active-phase algorithm for multimaterial topology optimization problems: a 115-line matlab implementation," *Structural and Multidisciplinary Optimization*, vol. 49, no. 4, pp. 621–642, 2014.

[13] H. A. Eschenauer, V. V. Kobelev, and A. Schumacher, "Bubble method for topology and shape optimization of structures," *Structural and Multidisciplinary Optimization*, vol. 8, no. 1, pp. 42–51, 1994.

[14] C. Fleury, "Conlin: an efficient dual optimizer based on convex approximation concepts," *Structural Optimization*, vol. 1, no. 2, pp. 81–89, 1989.

[15] K. Svanberg, "The method of moving asymptotesa new method for structural optimization," *International Journal for Numerical Methods in Engineering*, vol. 24, no. 2, pp. 359–373, 1987.

[16] Y. M. Xie and G. P. Steven, "A simple evolutionary procedure for structural optimization," *Computers & Structures*, vol. 49, no. 5, pp. 885–896, 1993.

[17] A. Tovar, "Bone remodeling as a hybrid cellular automaton optimization process," Ph.D. dissertation, University of Notre Dame, pp.1-2, 2004.

[18] A. Tovar, N. M. Patel, G. L. Niebur, M. Sen, and J. E. Renaud, "Topology optimization using a hybrid cellular automaton method with local control rules," *Journal of Mechanical Design*, vol. 128, no. 6, pp. 1205–1216, 2006.

[19] O. Sigmund, "A 99 line topology optimization code written in matlab," *Structural and multidisciplinary optimization*, vol. 21, no. 2, pp. 120–127, 2001.

[20] P. W. Christensen and A. Klarbring, *An introduction to structural optimization*. Springer Science & Business Media, 2008, vol. 153, pp. 1-2.

[21] O. Sigmund and J. Petersson, "Numerical instabilities in topology optimization: a survey on procedures dealing with checkerboards, mesh-dependencies and local minima," *Structural and Multidisciplinary Optimization*, vol. 16, no. 1, pp. 68–75, 1998.

[22] O. Sigmund, "Design of materials structures using topology optimization," Ph.D. dissertation, Department of Solid Mechanics, Technical University of Denmark, pp.1-2, 1994.

[23] M. Stolpe and K. Svanberg, "An alternative interpolation scheme for minimum compliance topology optimization," *Structural and Multidisciplinary Optimization*, vol. 22, no. 2, pp. 116–124, 2001.

[24] N. Wiener and A. Rosenblueth, "The mathematical formulation of the problem of conduction of impulses in a network of connected excitable elements, specifically in cardiac muscle." *Archivos del Instituto de Cardiología de México*, vol. 16, no. 3, pp. 205–265, 1946.

[25] A. W. Burks, *Essays on cellular automata*. University of Illinois Press, pp. 1-2, 1970.

[26] N. Inoue, N. Shimotai, and T. Uesugi, "Cellular automaton generating topological structures," in *Smart Structures and Materials: Second European Conference*. International Society for Optics and Photonics, 1994, pp. 47–50.

[27] E. Kita and T. Toyoda, "Structural design using cellular automata," *Structural and Multidisciplinary Optimization*, vol. 19, no. 1, pp. 64–73, 2000.

[28] O. Sigmund and S. Torquato, "Design of materials with extreme thermal expansion using a three-phase topology optimization method," *Journal of the Mechanics and Physics of Solids*, vol. 45, no. 6, pp. 1037–1067, 1997.

[29] J. Stegmann and E. Lund, "Discrete material optimization of general composite shell structures," *International Journal for Numerical Methods in Engineering*, vol. 62, no. 14, pp. 2009–2027, 2005.

[30] M. P. Bendsoe and O. Sigmund, *Topology optimization: theory, methods, and applications*. Springer Science & Business Media, pp. 1-2, 2013.

[31] O. Sigmund, "Design of multiphysics actuators using topology optimization–part ii: Two-material structures," *Computer Methods in Applied Mechanics and Engineering*, vol. 190, no. 49, pp. 6605–6627, 2001.

[32] W. Zuo and K. Saitou, "Multi-material topology optimization using ordered simp interpolation," *Structural and Multidisciplinary Optimization*, pp. 1–15, 2016.

[33] M. Y. Wang and X. Wang, "color level sets: a multi-phase method for structural topology optimization with multiple materials," *Computer Methods in Applied Mechanics and Engineering*, vol. 193, no. 6, pp. 469–496, 2004.

[34] S. Zhou and M. Y. Wang, "Multimaterial structural topology optimization with a generalized cahn–hilliard model of multiphase transition," *Structural and Multidisciplinary Optimization*, vol. 33, no. 2, pp. 89–111, 2007.

[35] A. Ramani, "A pseudo-sensitivity based discrete-variable approach to structural topology optimization with multiple materials," *Structural and Multidisciplinary Optimization*, vol. 41, no. 6, pp. 913–934, 2010.

[36] L. V. Gibiansky and O. Sigmund, "Multiphase composites with extremal bulk modulus," *Journal of the Mechanics and Physics of Solids*, vol. 48, no. 3, pp. 461–498, 2000.

[37] N. M. Patel, "Crashworthiness design using topology optimization," Ph.D. dissertation, University of Notre Dame, pp. 1-2, 2007.

[38] J. Fang, G. Sun, N. Qiu, N. H. Kim, and Q. Li, "On design optimization for structural crashworthiness and its state of the art," *Structural and Multidisciplinary Optimization*, pp. 1–29, 2016.

[39] R. R. Mayer, N. Kikuchi, and R. A. Scott, "Application of topological optimization techniques to structural crashworthiness," *International Journal for Numerical Methods in Engineering*, vol. 39, no. 8, pp. 1383–1403, 1996.

[40] C. B. Pedersen, "Topology optimization design of crushed 2d-frames for desired energy absorption history," *Structural and Multidisciplinary Optimization*, vol. 25, no. 5-6, pp. 368–382, 2003.

[41] C. Soto, "Structural topology optimization for crashworthiness," *International Journal of Crashworthiness*, vol. 9, no. 3, pp. 277–283, 2004.

[42] G.-J. Park, "Technical overview of the equivalent static loads method for nonlinear static response structural optimization," *Structural and Multidisciplinary Optimization*, vol. 43, no. 3, pp. 319–337, 2011.

[43] C. Chuang and R. Yang, "Benchmark of topology optimization methods for crashworthiness design," in *12th International LS-DYNA Users Conference, Dearborn, Michigan, USA*, 2012, pp. 1–2.

[44] N. M. Patel, B.-S. Kang, J. E. Renaud, and A. Tovar, "Crashworthiness design using topology optimization," *Journal of Mechanical Design*, vol. 131, no. 6, p. 061013, 2009.

[45] W. Roux, "Topology design using ls-tasc version 2 and ls-dyna®," 8th European LS-DYNA Users Conference, Strasbourg, France, pp. 1-2, 2011.

[46] K. Liu, A. Tovar, E. Nutwell, and D. Detwiler, "Towards nonlinear multimaterial topology optimization using unsupervised machine learning and metamodel-based optimization," in *ASME 2015 International Design Engineering Technical Conferences and Computers and Information in Engineering Conference*. American Society of Mechanical Engineers, 2015, pp. V02BT03A004–V02BT03A004.

[47] K. Liu, D. Detwiler, and A. Tovar, "Optimal design of nonlinear multimaterial structures for crashworthiness using cluster analysis," *Structural and Multidisciplinary Optimization*, pp. 1–10, 2017.